Charles University

Faculty of Science

Study program: Biology

Branch of study: Immunology

Bc. Petra Vávrová

The role of ORMDL3 in the IgE receptor signaling

Role ORMDL3 v signalizaci IgE receptoru

Diploma thesis

Supervisor: Mgr. Viktor Bugajev, Ph.D

Prague, 2020

Prohlášení:

Prohlašuji, že jsem diplomovou práci vypracovala samostatně, a že jsem uvedla veškerou použitou literaturu. Tato práce, ani její podstatná část nebyla předložena k získání stejného nebo jiného akademického titulu.

V Praze, 10. 8. 2020

Petra Vávrová

Acknowledgements

I would like to thank my supervisor Mgr. Viktor Bugajev, Ph.D for his guidance, advices and support and I would also like to express my gratitude to RNDr. Petr Dráber, DrSc for the chance to work in his laboratory. I would also like to thank all the other members of the Laboratory of Signal Transduction for their support and valuable advices. And my thanks also belong to people from core facilities of Institute of Molecular Genetics. Finally I would like to thank my family and friends for their endless love, support and encouragement during my studies.

Abstract

ORMDL proteins are regulators of serine palmitoyltransferase (SPT) enzyme, which catalyzes the first step of sphingolipid biosynthesis. Human and murine ORMDL family consists of three members, ORMDL1, ORMDL2 and ORMDL3. Human and murine ORMDLs exhibit high similarity between their amino acid sequences. ORMDL3 expression has been linked to several diseases, such as childhood-onset asthma, Crohn's disease, rheumatoid arthritis, type 1 diabetes, and primary biliary cirrhosis. High expression of ORMDL3 has been found in macrophages, T cells, eosinophils, epithelial cells and mast cells. ORMDL3 is a negative regulator of the high affinity IgE receptor I (FcεRI)-mediated signaling in mast cells. Mast cells have an important role in the acute phase of allergic reactions and are involved in eradication of multicellular parasites.

In the first part of this thesis we determined the expression of ORMDL family in peritoneal-derived mast cells (PDMCs) from *Ormdl3* knock out (KO) and wild type (WT) mice. Next we determined the roles of ORMD3 in FcεRI-mediated signaling in these PDMCs. Furthermore, we analyzed the relationship between expression of ORMDL family and SPT complex in bone marrow-derived mast cells (BMMCs) and bone marrow-derived mast cell line (BMMCL). We transduced BMMCL with vector coding SPTLC1 shRNA to induce SPTLC1 knock down (KD) and compared them with control BMMCL. Furthemore, we analyzed the expression of these proteins in BMMCs isolated from WT, *Ormdl2* KO, *Ormdl3* KO and *Ormdl2&3* double knock out (DKO) mice. In the final part of this thesis, we studied the role of ORMDL family in imiquimod (IMQ)-induced dermatitis, particularly in *Ormdl2* KO, *Ormdl3* KO, and *Ormdl2&3* DKO mice.

Keywords: ORMDL3, Mast cells, FcεRI, Imiquimod-induced skin inflammation

Abstrakt

ORMDL proteiny jsou regulátory serin palmitoyl transferázy (SPT), enzymu, který katalyzuje první krok v syntéze sfingolipidů. Lidská a myší ORMDL rodina se skládá ze tří členů, ORMDL1, ORMDL2 a ORMDL3, jejichž sekvence aminokyselin mají mezi sebou vysokou podobnost. ORMDL3 exprese je spojována s několika chorobami, jako je astma počínající v dětství, Crohnova choroba, revmatoidní artritida, diabetes 1. typu a primární biliární cirhóza. Vysoká exprese ORMDL byla nalezena u makrofágů, T buněk, eozinofilů, epiteliálních buněk a žírných buněk. ORMDL3 je negativní regulátor signalizace zprostředkované vysoce afinitním IgE receptorem I (FcεRI)v žírných buňkách. Ty hrají velmi důležitou roli v akutní fázi alergické reakce a při infekci mnohobuněčnými parazity.

V první části této práce jsme určili expresi ORMDL rodiny v žírných buňkách izolovaných z peritonea (PDMCs) *Ormdl3* knock out (KO) a wild type (WT) myší a dále jsme určili v těchto buňkách roli ORMDL3 v FcεRI signalizaci. V další části této práce jsme studovali vztah mezi expresí rodiny ORMDL a komplexem SPT v žírných buňkách derivovaných z kostní dřeně (BMMCs) a linii v žírných buněk odvozených z kostní dřeně (BMMCL). BMMCL jsme transdukovali vektorem kódujícím SPTLC1 shRNA, abychom indukovali SPTLC1 knock down (KD) a porovnali je s kontrolními BMMCL. Dále jsme analyzovali expresi těchto proteinů v BMMCs, které byly izolované z WT, *Ormdl2* KO, *Ormdl3* KO a *Ormdl2&3* double knock out (DKO) myší. V poslední části této práce jsme studovali roli ORMDL rodiny v imiquimodem indukované dermatitidě, konkrétně v *Ormdl2* KO, *Ormdl3* KO a *Ormdl2&3* DKO myších.

Klíčová slova: ORMDL3, žírné buňky, FcεRI, Imiquimodem indukovaný zánět kůže

Table of content

1 List of abbreviations

aa	Amino acid
ADAM	A disintegrin and metalloproteinase domain-containing protein
Ag	Antigen
AHR	Airway hyperresponsivness Bone-marrow
ATF6α	Activating transcription factor 6
BM	Bone-marrow
BMMC	Bone marrow-derived mast cell
BSS-BSA	Buffered saline solution with Bovine serum albumine
CD	Cluster of differentiation
CoA	Coenzyme A
COX2	Cyclooxygenase-2
DES1	Dihydroceramide desaturase-1
DKO	Double knock out
ER	Endoplasmic reticulum
FcεRI	High affinity IgE receptor I
HEK293	Human embryonic kidney 293 cells
IgE	Immunoglobulin E
IL	Interleukin
IMQ	Imiquimod
IκB-α	Inhibitor of nuclear factor kappa B
KD	Knock down
KO	Knock out
MMP9	Matrix metallopeptidase-9
MRGPRB2	Mas-related G-protein coupled receptor member B2
MRGPRX2	Mas-related G-protein coupled receptor member X2
NF-κB	Nuclear factor NF-kappa-B
ORMDL	ORM1-like protein
OVA	Ovalbumine
p/ERK	Phosphorylated / Extracellular signal-regulated protein kinase
PDMC	Peritoneal-derived mast cells
PGD2	Prostaglandin D2
PRR	Pattern recognition receptor

S1P	Sphingosine-1phosphate
$S1P_{1/2}$	S1P receptors on mast cells
SCF	Stem cell factor
SDS	Sodium dodecyl sulfate
SERCA2B	Sarcoplasmic/endoplasmic reticulum calcium-ATPase 2
SNP	Single-nucleotide polymorphism
SPHK	Sphingosine kinase
SPT	Serine palmitoyltransferase
SPTLC	SPT light chain
TNF-α	Tumor necrosis factor-α
TNP	Trinitrophenyl
UPR	Unfolded protein response
WT	Wild type

2 Introduction

2.1 ORMDL family

ORMDL proteins are regulators of serine palmitoyltransferase (SPT), an enzyme which catalysis sphingolipid biosynthesis (Breslow et al., 2010; Davis et al., 2019b). Sphingolipids constitute a branched family of lipids comprising critical structural components of cellular membranes and lipid signaling mediators (Hannun and Obeid, 2008; Wennekes et al., 2009).

Human ORMDL family consists of three members, *ORMDL1, ORMDL2 and ORMDL3*, which are localized on chromosomes 2q32, 12q13.2 and 17q21, respectively. Murine *Ormdl1, Ormdl2* and O*rmdl3* are localized on chromosomes 1, 10 and 11, respectively. The members of human and murine ORMDL family are small proteins of 153 amino acids (aa) that span the endoplasmic reticulum (ER) membrane four times (Fig. 1A; Hjelmqvist et al., 2002, Davis et al., 2019a). Orthologues of ORMDL family have been reported in plants, urochordates, yeast, microsporidia, invertebrates and vertebrates, but are missing in *Caenorhabitis elegans,* although in other nematode species they are present (Hjelmqvist et al., 2002).

When the aa sequences of different ORMDL families were compared, a high similarity between them was found, especially in vertebrates. For example, similarity between human (h)ORMDL1 and murine (m)ORMDL1 is higher (99%) than between hORMDL1 and hORMDL2 (83%) or hORMDL1 and h/mORMDL3 (84%). The comparison of aa sequences between mORMDL2 and mORMDL3 (83%) is shown in Figure 1B. However, similarity between sequences of hORMDLs compared with sequences of ORM orthologues from *Arabidopsis thaliana* or different Orm-1-like yeast species are approximately between 30–40% (Hjelmqvist et al., 2002).

A

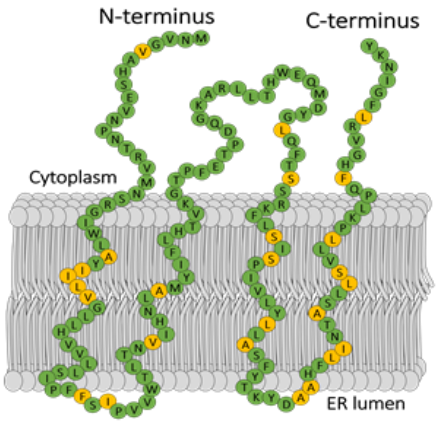

B

```
mORMDL2     1  MNVGVAHSEVNPNTRVMNSRGIWLAYIILVGLLHVVLLSI  40
mORMDL3     1  MNVGTAHSEVNPNTRVMNSRGIWLSYVLAIGLLHVVLLSI  40

mORMDL2    41  PFFSIPVVWTLTNVIHNLAMYIFLHTVKGTPFETPDQGKA  80
mORMDL3    41  PFVSVPVVWTLTNLIHNLGMYIFLHTVKGTPFETPDQGKA  80

mORMDL2    81  RLLTHWEQMDYGLQFTSSRKFLSISPIVLYLLASFYTKYD  120
mORMDL3    81  RLLTHWEQMDYGVQFTASRKFLTITPIVLYFLTSFYTKYD  120

mORMDL2   121  AAHFLINTASLLSVLLPKLPQFHGVRLFGINKY  153
mORMDL3   121  QVHFILNTVSLMTVLIPKLPQLHGVRIFGINKY  153
```

Fig. 1: T Topology of mORMDL2 and comparison of aa sequences of ORMDL2 and ORMDL3.

(A) Predicted topology of murine ORMDL2 based on recently described ORMDL1 topology (Davis et al., 2019a). Residues marked in the murine ORMDL2 by green color indicate conserved amino acids, in yellow are shown residues which are in murine ORMDL3 different. (B) The comparison of primary aa sequences of murine ORMDL2 and ORMDL3. The sequences were aligned using DNASTAR Lasergene 15 (Bugajev et al., manuscript in preparation).

2.1.1 ORMDL-dependent regulation of sphingolipid biosynthesis

Sphingolipids are a wide family of lipids that includes ceramides, glycosphingolipids, sphingosines and sphingomyelin (Mandon et al., 1991). They are important structural glycolipids in cell membranes, which modulate cellular events, such as differentiation, proliferation and apoptosis (Hannun and Luberto, 2000). They also function as signal molecules and, together with cholesterol, they can form membrane microdomains, which are known as lipid rafts (Futerman and Hannun, 2004). All of them are derived by alteration of a long-chain base sphingolipid backbone. The crucial step of *de novo* production of the long-chain base sphingolipid backbone is catalyzed by SPT (Mandon et al., 1991; Breslow et al., 2010; Siow et al., 2015). The SPT enzyme is composed of SPTLC1 subunit, which pairs with SPTLC2 or SPTLC3 subunit to form a heterodimeric complex (Hanada, 2003; Harrison et al., 2018). In mammals were also found two additional smaller subunits (ss)SPTa and ssSPTb (Han et al. 2009). The SPT complex is located at the cytosolic leaflet of the ER membrane (Hanada, 2003) and catalyzes the condensation of a fatty acetyl coenzyme A (acyl-CoA; mostly palmitoyl-CoA) and an amino acid (mostly serine; Mandon et al., 1991; Breslow et al., 2010; Siow et al., 2015). The resulting metabolite, 3-ketodihydrosphingosine, is quickly transformed to dihydrosphingosine (sphinganine; Hanada, 2003; Lowther et al., 2012; Wills-Karp, 2020). Sphinganine is further metabolized to dihydroceramide by distinct ceramide synthases. Subsequently, dihydroceramide desaturase-1 (DES1) converts dihydroceramide to ceramides (Fig. 2; Wills-Karp, 2020). Ceramides are transported out of the ER in order to form complex glycosphingolipids or sphingomyelins. These sphingolipids can be recycled in lysosomes back to ceramides in order to maintain physiologic concentrations of sphingolipids in the cell membranes (Fig.2). Ceramides can also be phosphorylated by ceramide kinase to form ceramide-1-phosphate, a signaling molecule, or metabolized by ceramidase to sphingosine. Sphingosine is converted back to ceramide by ceramide synthases or used as a substrate of sphingosine kinases (SPHK) to produce sphingosine-1-phosphate (S1P), another potent bioactive lipid (Fig. 2; Hanada, 2003; Lowther et al., 2012; Wills-Karp, 2020).

Breslow et al. identified proteins Orm1 and Orm2 as negative regulators of the yeast SPT (Lcb1 and Lcb2). The increased expression of Orm1 or Orm2 reduced the sphingolipid levels. In concordance, the absence of Orm1/2 in yeast resulted in toxic accumulation of sphingolipids. Moreover, the Orm1/2-mediated regulation of sphingolipid biosynthesis was found to be associated with phosphorylation of Orm1/2. Interestingly, the whole N-terminal part of Orm1/2 proteins comprising the phospho-specific residues, which are involved in Lcb1/2 regulation, is missing in mammalian ORMDL family. However, the silencing of all three ORMDL family members caused accumulation of ceramide levels in HeLa cells. ORMDL3 tagged with FLAG also interacted with SPTLC1 subunit of SPT in HEK293 T cells (Breslow et al., 2010). Recently, it was demonstrated, that the inhibition of SPT via ORMDL in mammalian cells is strictly dependent on the native D-erythro stereoisomer of ceramide. This indicates that ceramide directly binds to the ORMDL regulatory apparatus and mediates feedback inhibition of SPT in the conditions of increased ceramide levels (Davis et al., 2019b).

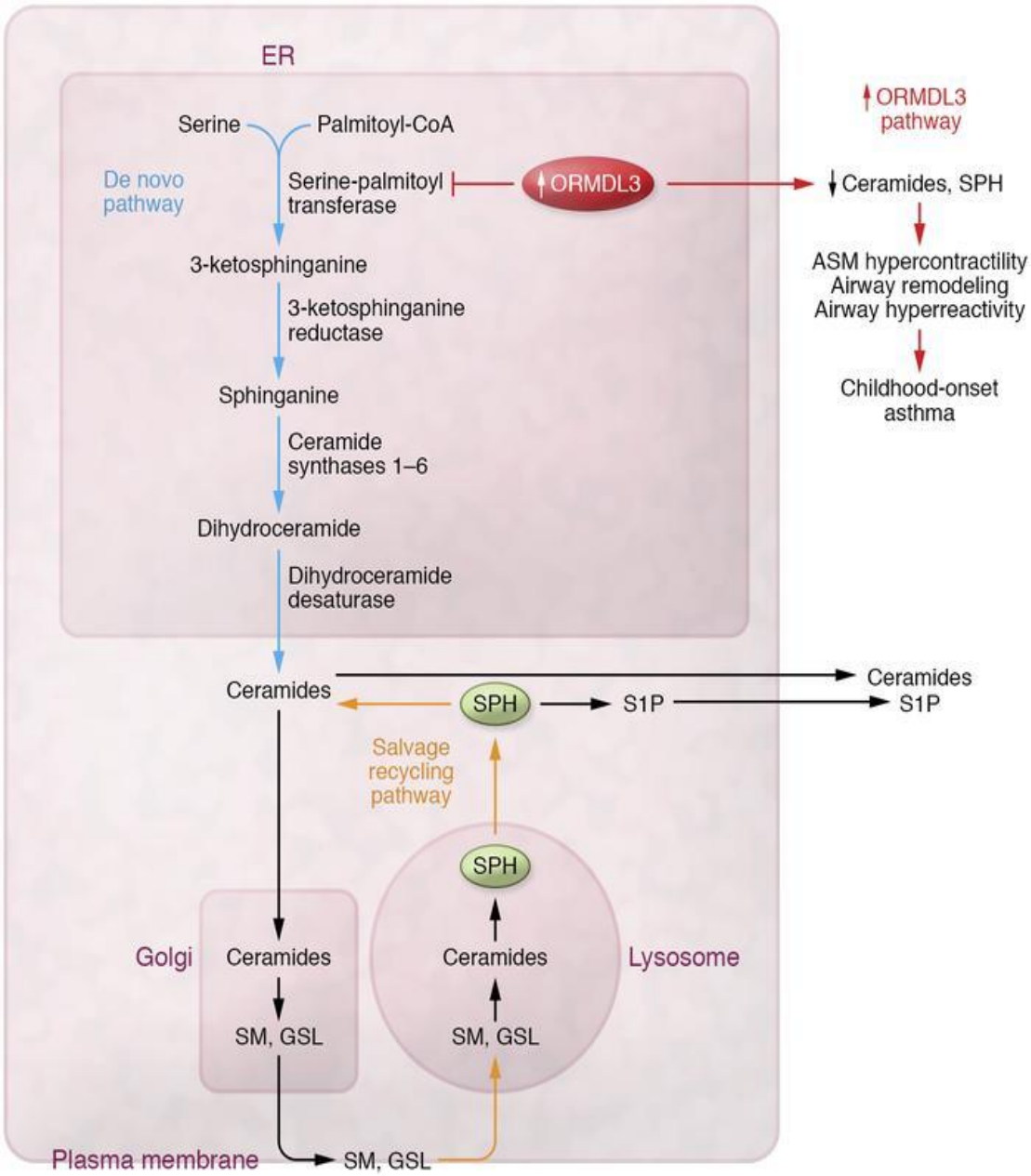

Fig. 2: The role of ORMDL3 in sphingolipid biosynthesis pathway and childhood-onset asthma.

The first step in *de novo* sphingolipid synthesis is condensation of serine and palmitoyl-CoA catalyzed by SPT leading to 3-ketosphinganine production. 3-ketosphinganine is rapidly transformed to dihydrosphingosine (sphinganine), which is then metabolized to dihydroceramide via distinct ceramide synthases. Subsequently, dihydroceramide desaturase-1 (DES1) transforms dihydroceramide to ceramide. Ceramides are transported out of the ER to Golgi, where they are further transformed into complex sphingomyelins (SM) or glycosphingolipids (GSL). These sphingolipids can be transported to lysosomes, where are recycled back to ceramides. Ceramide can be phosphorylated to ceramide-1-phospate by ceramide kinase (not shown) or metabolized to sphingosine (SPH) via ceramidase. Sphingosine can be transformed by ceramide synthases into ceramide or it can be used as a substrate of sphingosine kinases to produce sphingosine-1-phosphate (S1P). Increased expression of ORMDL3 reduces *de novo* synthesis of sphingolipids. This reduction was associated with properties of childhood onset asthma such as airway smooth muscle (ASM) hypercontractility, airway hyperreactivity and airway remodeling (Adapted from Wills-Karp, 2020).

2.1.2 The redundancy of ORMDL function

As was mentioned in chapter 2.1.1, mammalian ORMDLs inhibit *de novo* synthesis of sphingolipids. To understand the function of ORMDLs *in vivo*, Clarke et al., (2019) prepared whole-body *Ormdl1* KO, *Ormdl2* KO, and *Ormdl3* KO mice. Moreover, double KO combinations were established (*Ormdl1&2* DKO, *Ormdl1&3* DKO, and *Ormdl2&3* DKO mice). A neurologic phenotype in *Ormdl1&3* DKO, which was determined by forelimb wire hang behavioral test suggested the function of ORMDL1 and ORMDL3 in brain development. Indeed, the levels of dihydroceramide, dihydrosphingosine, ceramide and sphingosine in brains of these mice were elevated when compared with WT, *Ormdl1* KO, *Ormdl2* KO and *Ormdl1&2* DKO. In the brains of *Ormdl3* KO mice, the levels of these sphingolipids were also increased when compared with WT mice but less than in *Ormdl1&3* DKO. The redundant levels of myelin in sciatic nerve of *Ormdl1&3* DKO mice caused their improper myelination associated with abnormal morphology and reduced the amount of myelinated axons. The combined data suggests that ORMDL3 has the largest impact on *de novo* sphingolipid synthesis in mouse brain among all ORMDL family members. Moreover, ORMDL1 and ORMDL3 function redundantly to control the proper myelination of the nerves (Clarke et al., 2019).

2.2 ORMDL3-specific function

2.2.1 ORMDL3 in diseases

ORMDL3 has been extensively studied since 2007, when single-nucleotide polymorphisms (SNPs) in chromosomal region 17q12-q21 of patients with childhood-onset asthma were associated with decrease in *ORMDL3* expression (Moffatt et al., 2007). Recently, *Ono et al.* confirmed that asthma-risk genotypes in children with low-eosinophil-count asthma (non-allergic asthma) are related to the lower levels of dihydroceramides, ceramides, and sphingomyelins in the whole-blood cells. They also reported that children with high-eosinophil counts (allergic asthma) in contrast to non-allergic asthma exhibited comparable levels of ceramides, dihydroceramides and sphingomyelins with healthy subjects (Ono et al., 2020). Further studies also linked the changes in ORMDL3 expression to the SNPs in the 17q12-q21 region associated with type 1 diabetes, Crohn's disease, primary biliary cirrhosis and rheumatoid arthritis (Verlaan et al., 2009; Kurreeman et al., 2012).

2.2.2 ORMDL3 in mouse models

Transgenic mice hORMDL3$^{zp3\text{-}Cre}$, which ubiquitously overexpressed human ORMDL3 under zona pellucida promoter, exhibited increased levels of IgE in serum. They developed spontaneously enhanced airway remodeling leading to subepithelial fibrosis and increased mucus production, which resulted to increased airway hyperresponsivness (AHR) to methacholine. This corresponded to an enhanced amount of macrophages, neutrophils, eosinophils and $CD4^+$ T cells in the lungs of these mice compared with WT mice. They also exhibited increased levels of Th2 cytokines (Miller et al., 2014). In line with these findings, *Ormdl3* KO mice were protected from developing of AHR induced by *Alternaria alternata* allergen (Löser et al., 2017). Moreover, intranasal administration of a mix of vectors containing shRNAs targeting *Ormdl3* mRNA decreased the ovalbumin (OVA) allergen-induced AHR in mice (Dileepan et al., 2020). However, mice with conditionally targeted *Ormdl3* gene in the lung epithelia, prepared by crossing *Ormdl3*^{loxP} mice with *CC10-Cre*^{tg} mice, exhibited OVA allergen-dependent increase in AHR. The authors reported that this enhanced AHR was associated with elevated S1P levels (Miller et al., 2017). It should be noted, that Debeuf et al., independently prepared mice with reduced or enhanced ORMDL3 levels, in which found the changes in sphingolipid levels without any differences in all key asthma parameters in allergen-induced AHR (Debeuf et al., 2019).

2.2.3 Cell-type dependent role of ORMDL3

The understanding of ORMDLs-dependent inhibition of sphingolipid biosynthesis was important for further studies elucidating the role of these proteins in distinct cell types. The exposure of the cells to stressors, such as chemotherapeutic agents or cell activators induces the unfolded protein response (UPR) followed by *de novo* ceramide synthesis (Perry, 2000; Kiefer et al., 2015). The changes in expression of ORMDL family are also associated with UPR (Miller et al., 2012).

High expression levels of ORMDL3 were found in eosinophils, macrophages, T cells, lung epithelial cells, and mast cells (Fig. 3; Miller et al., 2012; Ha et al., 2013; Schmiedel et al., 2016, Bugajev 2016)

2.2.3.1 ORMDL3 in epithelial cells

ORMDL3 is expressed in mouse lungs, especially in airway epithelial cells. WT mice stimulated with allergens exhibited increased *ORMDL3* mRNA expression in bronchial epithelial cells (Miller et al., 2012).

In human bronchial epithelial cells, increased levels of ORMDL3 induces expression of a disintegrin and metalloproteinase domain-containing protein 8 (ADAM8) (Miller et al., 2012), which belongs to the zinc protease superfamily (Seals and Courtneidge, 2003). ADAM8 has an important role in the release of membrane-bound cytokines or mediators and contributes to the airway remodeling followed by development of airway inflammation (Naus et al., 2010; Paulissen et al., 2011).

Overexpression of ORMDL3 in bronchial epithelial cells also resulted in increased expression of matrix metalloproteinase 9 (MMP9; Miller et al, 2012). MMP9 is an enzyme, which is capable of degrading the extracellular matrix. Increased expression of MMP9 was found in bronchial biopsies from patients with asthma (Ohno et al., 1997). MMP9-deficient mice exhibited decreased OVA allergen-induced airway inflammation accompanied by attenuated airway remodeling (Lim et al., 2006).

Upregulation of ORMDL3 in lung epithelium activates an activating transcription factor 6 (ATF6α). This transcription factor induces expression of *Atp2a2,* a gene coding Sarcoplasmic/endoplasmic reticulum calcium-ATPase 2 (SERCA2b). SERCA2b is a calcium pump that transfers cytosolic Ca^{2+} to the lumen of the ER. Changes in Ca^{2+} homeostasis induces subepithelial fibrosis followed by AHR (Fig. 3a; Miller et al., 2012).

2.2.3.2 ORMDL3 in Eosinophil

Eosinophils are granulocytes, which migrate to the lung tissues during allergic inflammation. The high-eosinophil-count-associated asthma (allergic asthma) is linked to airway remodeling and AHR (Possa et al., 2013; Ono 2020). The *Ormdl3* expression in bone marrow (BM)-derived eosinophils is induced by eotaxin-1 or IL-3 (Fig. 3B; Ha et al., 2013). These signaling molecules are responsible for recruitment and proliferation of eosinophils (Hamid and Tulic, 2009). BM-derived eosinophils with enhanced ORMDL3 expression exhibited the increased translocation of the transcription factor NF-κB into nuclei followed by elevated expression of the adhesion molecules and cytokines compared with control cells. ORMDL3-GFP expression in BM-derived eosinophils also caused cytoskeletal rearrangement and enhanced rolling of murine eosinophils on mVCAM-1-coated cover-slips compared with cells expressing GFP alone. On the other hand, ORMDL3 KD in BM-derived eosinophils limits cell polarization, spreading, migration, and CD48-mediated degranulation (Ha et al., 2013).

2.2.3.3 ORMDL3 and T Cells

Schmiedel et al., (2016) showed that *ORMDL3* is highly expressed in most primary immune cells except dendritic cells and monocytes. Naïve $CD4^+$ T cells, which were collected from subjects with SNPs in the 17q21 region (asthma-risk allele), exhibited an increased expression of ORMDL3 compared with samples from subjects without the asthma-risk allele. Isolated $CD4^+$ T cells were transiently transfected with siRNA pools specific for *ORMDL3* or non-targeting siRNA and activated *ex vivo* using CD3 and CD28 antibodies. The increased levels of IL-2 in $CD4^+$ T cells with ORMDL3 KD compared with control cells suggested that ORMDL3 is a negative regulator of IL-2 production in $CD4^+$ T cells (Fig. 3C; Schmiedel et al., 2016).

2.2.3.4 ORMDL3 in macrophages

BM-derived macrophages isolated from *hORMDL*^{Rosa26} transgenic mice exhibited decreased levels of ceramide and toll-like receptor 4-mediated autophagy compared with WT mice (Kiefer et al., 2019).

2.2.3.5 ORMDL3 in mast cells

Mast cells play a crucial role in IgE-dependent allergic disorders (Galli et al., 2008). The FcεRI-mediated activation of BMMCs with ORMDL3 KD enhanced phosphorylation and degradation of IκB-α, which was followed by increased translocation of the NF-κB p65 subunit into the nucleus. Subsequently, the expression of chemokines (CCL3 and CCL4), proinflammatory cytokines (TNF-α, IL-6, and IL-13), and cyclooxygenase-2 (COX-2) was increased in BMMCs with ORMDL3 KD compared with control cells. The increased production of COX2 was accompanied by enhanced levels of prostaglandin D2 (PGD2) in BMMCs with ORMDL3 KD (Fig. 3D; Bugajev et al., 2016).

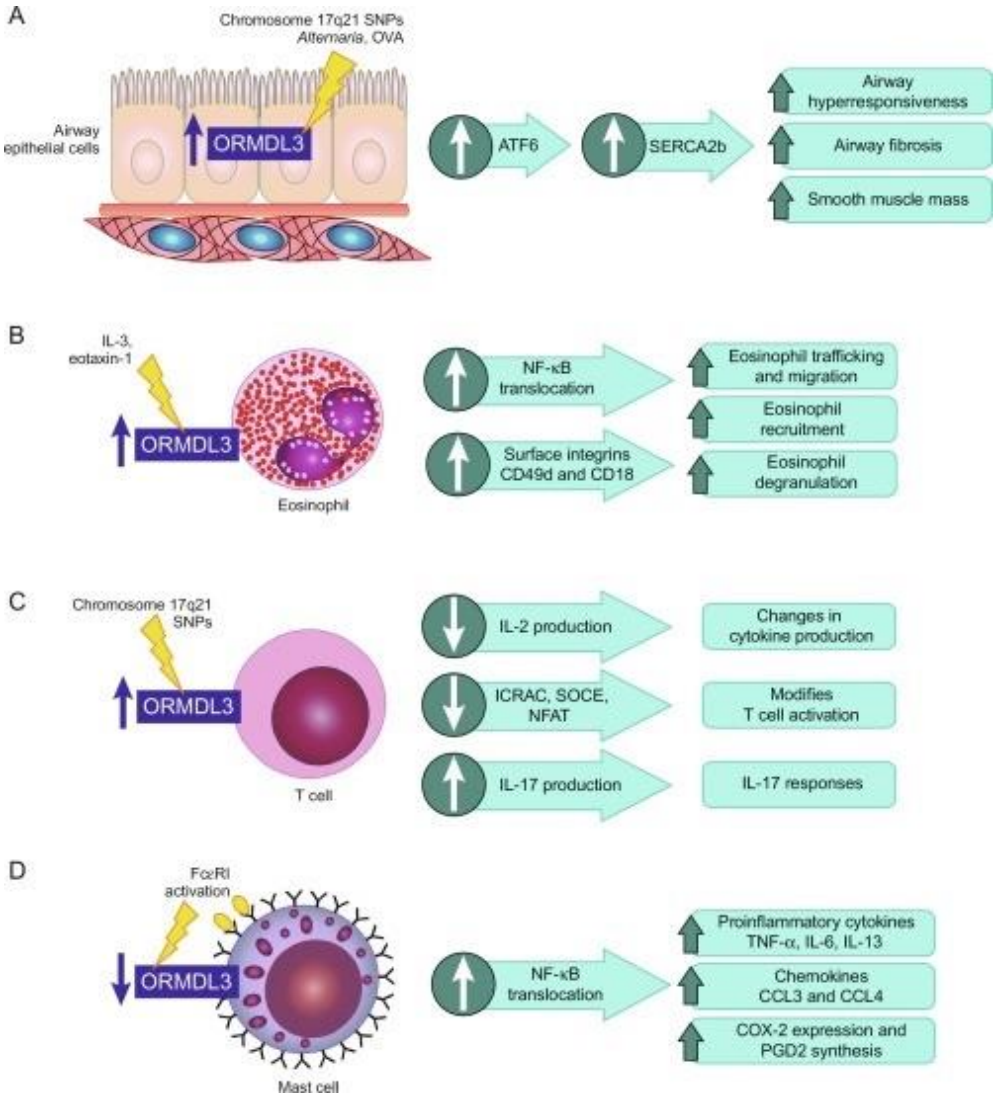

Fig. 3: ORMDL3-dependent regulation in different type of cells.
A) ORMDL3 in epithelial cell – upregulation of ORMDL3 can be driven by SNPs on chromosome 17q21 or allergens (OVA, *Alternaria alternata*). Increased expression of ORMDL3 can activate one of the branches of the UPR pathway like activating transcription factor 6 (ATF6α). This factor increases expression of *Atp2a2* gene coding Sarcoplasmic/endoplasmic reticulum calcium-ATPase 2(SERCA2B) a calcium pump that transfers Ca^{2+} from the cytoplasm to the lumen of the ER. Changes in Ca^{2+} homeostaisis upregulates smooth muscle mass, subepithelial fibrosis and AHR. **B) ORMDL3 in eosinophil** – upregulation of ORMDL3 can be induced by IL-3 and eotaxin-1. Increased expression of ORMDL3 in eosinophil enhances NF-κB translocation to the nucleus and surface expression of integrins CD49d and CD18. These actions can result into increased eosinophil recruitment, trafficking, migration, and degranulation. **C) ORMDL3 in T cell** – upregulation of ORMDL3 can be induced by SNPs on chromosome 17q21. Increased expression of ORMDL3 can negatively regulate production of IL-2, store-operated calcium entry (SOCE), Ca^{2+} release-activated Ca^{2+} current (ICRAC), and nuclear factor of activated T cells (NFAT). These regulation leads to changes in cytokine production and modification of T cell activation. However increased expression of ORMDL3 can lead to increased production of IL-17 and IL-17-dependent signaling. **D) ORMDL3 in mast cell** – downregulation of ORMDL3 can be induced by FcεRI during mast cell activation. Decreased expression of ORMDL3 induces NF-κB translocation followed by enhanced production of proinflammatory cytokines, chemokines, cyclooxygenase (COX-2) and PGD2 synthesis Yellow lightening means induction; blue, white and green arrows denote upregulation or downregulation (Adapted and modified from Das et al., 2017).

2.3 Mast cells

Mast cells were first described in 1878 by Paul Ehrlich. In 1952, JF Riley and GB West reported that histamine is present in mast cells, which supported the hypothesis, that there is a relationship between histamine, mast cells and anaphylaxis (reviewed in da Silva et al., 2014). Mast cells originate from multipotent $CD13^{+}CD34^{+}CD117^{+}$ hematopoietic stem cells, which are located in the BM. Mast cell progenitors circulate in peripheral blood and migrate to tissues, where they differentiate and mature (Arinobu et al., 2005). Murine mast cells depend on two main growth factors, interleukin 3 (IL-3) and stem cell factor (SCF), a ligand for stem cell growth factor receptor Kit, which is the receptor tyrosine kinase. These growth factors are important for regulation of mast cell growth, survival and maturation (Tsai et al., 1991).

Mast cells, as a part of the innate immune system, rapidly participate in the organism's response to endogenous danger signals and to exogenous pathogens (Bischoff, 2007). Mast cells can be stimulated and activated by cytokines, toxins, neuropeptides, complement, growth factors, immune complexes, basic compounds, certain drugs and also by physical stimuli (Tkaczyk et al., 2004; Gilfillan et al., 2009). The activation of mast cells by allergens is the most commonly studied method. This type of activation, which depends on the adaptive immune response, is mediated by FcεRI that is located on the surface of mast cells (Galli et al. 2005).

Mast cell are found in skin, mucosal, and vascular barriers, which are the most exposed parts of body to the environment. Mast cells are located close to nerves and blood vessels, which allows them to react rapidly to various stimuli (Fig. 4; Marshall, 2004; Bischoff, 2007). Despite the fact that mast cells are not in direct contact with antigen presenting cells, they are able to modulate functions of antigen presenting cells via releasing a variety of mediators, including tumor necrosis factor-α (TNF-α; Kunder et al., 2009).

In summary, mast cells are leucocytes derived from myeloid lineage that have an important role in initiating immune responses to different types of pathogens, including viruses and bacteria. After activation, they promote inflammation. Therefore, better understanding of molecular mechanisms leading to mast cells-dependent inflammation is crucial to treat allergies and life-threatening anaphylactic shock.

.

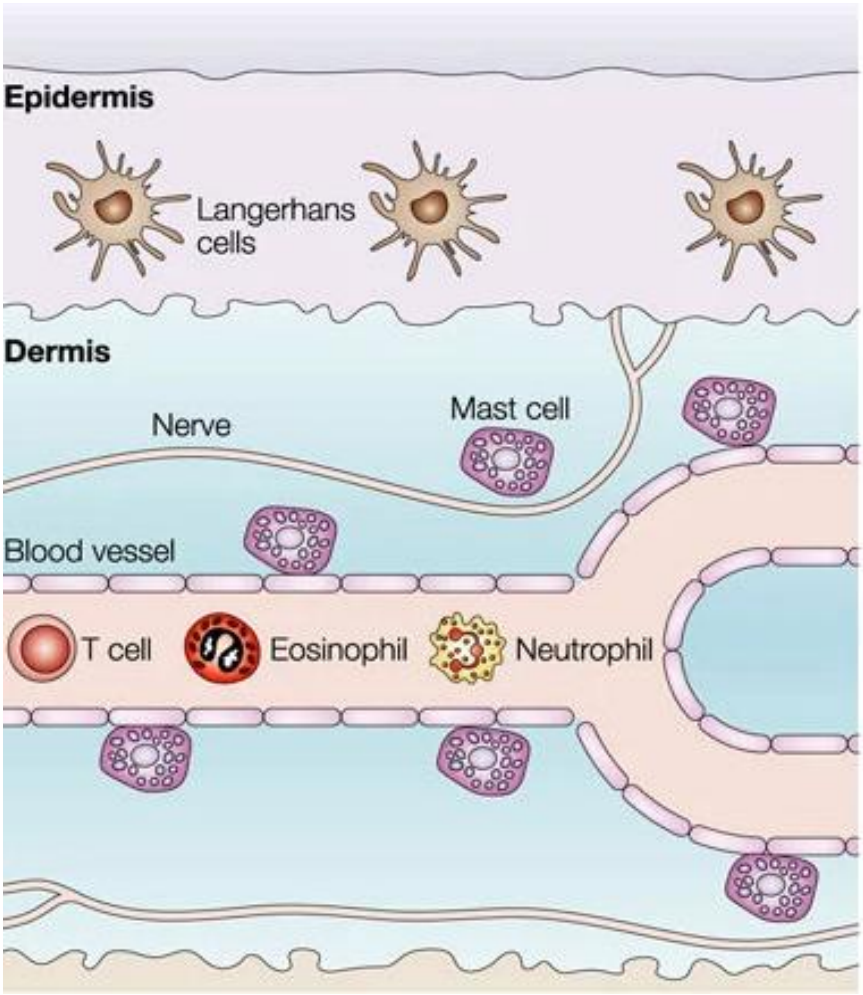

Fig. 4: Localization of mast cells in the tissue.
Mast cells are located in tissues, which are exposed to the external environment. They are also in the vicinity of nerves and blood vessels (Marshall, 2004).

2.3.1 Mast cells and receptors

Mast cells express a large number of receptors. They are activated for example through recognition of pathogen-associated molecular patterns by pattern recognition receptors (PRRs). Mast cells possess distinct membrane-bound Toll-like receptors, belonging to the family of PRRs. The interaction between specific pathogen-associated molecular patterns with PRRs causes the selective release of mediators by mast cells (Marshall, 2004).

Mast cells are crucial in development of allergy and anaphylactic shock. This reaction is mediated via FcεRI which is located on the surface of mast cell (Galli et al., 2005).

2.3.1.1 FcεRI

FcεRI belongs to the immunoglobulin receptor superfamily. It is a heterotetramer composed of the α, β, and γ_2 subunits. The α subunit binds to the Fc part of IgE, and the β and γ subunits contain on their cytoplasmic side immunoreceptor tyrosine-based activation motifs. The activation of mast cells through FcεRI is best characterized and most studied pathway in mast cells (Galli et al., 2005,). The process of activation depends on Ag-specific IgE (Kinet, 1999). The binding of multivalent antigens (Ag) to the FcεRI-IgE complex on the surface of the mast cell induces FcεRI crosslinking followed by triggering of intracellular signaling (Kovářová et al., 2001).

The signaling cascade of the FcεRI is composed of four cellular processes such as protein phosphorylation, intracellular calcium mobilization, lipids metabolism, and activation of transcription factors, resulting in cytokine production, production of lipid mediators and degranulation (reviewed in Tkaczyk et al., 2006 and Gilfillan and Tkaczyk; 2006).

2.3.1.2 Mas-related G-protein coupled receptor member X2 (MRGPRX2)

The MRGPRX2 is a human G-protein coupled receptor. The orthologue of this receptor in mice is MRGPRB2. MRGPRB2 activates mouse mast cells *in vivo* and *in vitro* via basic secretagogues and promotes pseudo-allergic inflammation. MRGPRB2-deficient mice exhibit decreased pseudo-allergic responses to various secretagogues compared with WT mice (McNeil et al., 2015).

The imiquimod (IMQ)-induced dermatitis was recently connected with the mast cells activation (Hao et al., 2020). Injection of IMQ into the footpad of WT mice caused its swelling and degranulation of mast cells determined by histamine release. Interestingly, *MrgprB2* KO mice exhibited reduced pseudo-allergy reaction in IMQ-induced dermatitis compared with WT mice. PDMCs isolated from *MrgprB2* KO mice exhibited decreased secretion of histamine, β-hexosaminidase, CXCL-2, and MCP1 compared with control cells. These data suggest that IMQ triggers MRGPRB2-dependent signaling in mast cells *in vitro* and *in vivo* (Hao et al., 2020).

2.3.2 The role of sphingolipids in mast cells

S1P is a bioactive lipid mediator derived from sphingosine. The production of S1P intracellularly mediates SPHK1 and SPHK2 by sphingosine phosphorylation (Olivera, 2008). Ag-stimulated mast cells generate and release S1P. S1P controls function of critical mast cell receptors for S1P. Two out of five receptors for S1P ($S1P_1$ and $S1P_2$ receptors) are expressed on mast cells. It has been shown that the activation of SPHKs and $S1P_1$ signaling participates in mast cells migration toward to Ag (Jolly et al., 2004). Moreover, the mast cell-dependent release of histamine in mice induces the negative regulatory feedback in passive systemic anaphylaxis, based on increased production of S1P, independent of mast cells, which in turn leads to the clearance of plasma histamine and attenuation of anaphylactic reaction (Olivera et al., 2010).

3 Aims

Aims of this diploma thesis were:

Aim 1: To determine the role of ORMDL3 in peritoneal-derived mast cells (PDMCs) isolated from WT or *Ormdl3* KO mice.

Aim 2: To analyze the relationship between expression of ORMDL family and SPT complex.

Aim 3: To study the role of ORMDL family in IMQ-induced dermatitis.

4 Materials and Methods

4.1 Cell cultures

Peritoneal derived mast cells (PDMCs) were isolated after washing murine peritoneum of WT and *Ormdl3* KO mice with 15 ml of culture medium. The cells were cultured in RPMI 1640 medium supplemented with antibiotics (100 μg/ml streptomycin; 100 U/ml penicillin), MEM non-essential amino acids, 71 μM 2-ME, 0.7 mM sodium pyruvate, 12 mM D-glucose, 2.5 mM L-glutamine, 10% fetal bovine serum and 4% WEHI-3 culture supernatant as a source of IL-3 and 4% culture supernatant from Chinese hamster ovary cells transfected with the cDNA encoding murine SCF, a kind gifts of Dr. P. Dubreuil; INSERM, Marseille, France. Peritoneal derived mast cells were grown for 2 weeks and then they were used for the experiments.

BM-derived mast cells (BMMCs) were derived from tibias and femurs of 8-to-10-week-old C57BL/6J WT, *Ormdl2* KO, *Ormdl3* KO, and *Ormdl2&3* DKOmice. The same medium was used as it was for PDMCs. After 8 weeks of cultivation ~99% cells were identified as mast cells based on FcεRI and c-KIT expression and then used within 2 months for the experiments.

A stable cell line derived from BM-derived mast cells (BMMCL) of C57BL/6 origin was donated by Dr. M. Hibbs (Ludwig Institute for Cancer Research, Melbourne, Australia). The cells were cultured in RPMI-1640 supplemented as above except that SCF was omitted. The transduction of BMMCL was performed by V. Bugajev.

All mice were maintained, and used in accordance with the Institute of Molecular Genetics guidelines (permit number 12135/2010-17210) and national guidelines (2048/2004-1020). Mice were kept under specific pathogen-free conditions and provided with food and water ad libitum.

4.2 Immunoblotting

Whole-cell lysates were prepared by washing the cells by cold phosphate-buffered saline (PBS), solubilizing them in hot sodium dodecyl sulfate (SDS)-sample buffer, sonicating 3 times for 20 s and then boiling the samples for 5 min. Protein extracts (30 µg) were aline with 4% stacking SDS-PAGE gel and separated on 13.5% SDS-PAGE gels. As a molecular weight marker was used a standard protein mix - Dual color marker (10-250 kDa). The apparatures for the protein separation were submerged into 1x electrode buffer. Separated protein extracts were electrophoretically transferred onto nitrocellulose membrane (GE Healthcare Life Sciences) using Bio-rad Mini-PROTEAN apparatus with constant setting 70 V for 90 min. The whole apparatus was dipped into transfer buffer. The membranes were blocked with 2% BSA-TNT solution (20 mM TRIS-HCl pH 7.5, 200 mM NaCl, 0.1% Tween) for one hour. Washed in protein- or phosphoprotein-specific antibodies for one hour and then washed three times per 5 min in TNT solution. Bound primary antibodies were detected with solution of 5% milk and HRP-goat anti-rabbit IgG or HRP-conjugated goat anti-mouse IgG secondary antibodies. HRP signal in phosphorylation and loads was developed with chemiluminescence reagent ECL and quantified by Luminescent Image Analyzer LAS 3000 (Fuji Photo Film Co.). Aida software (Raytest GmbH) was used for signal quantification.

Reagents	Con.	4% stacking gel	13,5% separating gel
Tris pH 6.8	0.5 M	0.625 ml	
Tris pH 8.8	1.5 M		2.5 ml
Polyacrylamide mix		0.325 ml	4.5 ml
10% SDS		0.025 ml	0.1 ml
Ammonium presulfate		0.0125 ml	0.05 ml
TEMED		0.0025 ml	0.005 ml
dH2O		1.525 ml	2.85 ml

Table 1: SDS-PAGE gels

Reagents	Volume/Weight
Trizma ® base	33 g
Glycine	144 g
methanol	1 L

Table 2: Transfer buffer

Reagents	Volume/weight
Trizma ® base	60 g
Glycine	288 g
Sodium dodecyl sulfate	20 g
dH_2O	2 L

Table 3: 10x Electrode buffer

Reagents	Con.	Volume
Tris pH 7.5	1 M	10 ml
NaCl	5 M	20 ml
Tween		1 ml
dH_2O		969 ml
Final volume		1 L

Table 4: TNT solution

Reagents	Volume/weight
BSA	1 g
TNT	Fill up to 50 ml

Table 5: 2% BSA-TNT solution

Reagents	Volume/weight
Skimmed milk	2.5 g
TNT solution	Fill up to 50 ml

Table 6: 5% milk solution

Reagents	Con.	Volume
Tris for ECL pH 8.8	0.1 M	20 ml
Luminol	240 mM	100 µl
Couramic acid	40 mM	100 µl
H_2O_2		4 µl

Table 7: chemiluminescence reagent ECL

4.3 β-Glucuronidase release and Ca^{2+} response

Mast cells were sensitized in SCF- and IL-3-free culture medium with TNP-specific IgE (IGEL b4 1 mAb; obtained from Dr. A. K. Rudolph; Rudolph et al., 1981). The cells were washed after 16 hours and aliquoted into 96-well plate ($1.5x10^5$ in 30 µl/well) in BSS supplemented with 0.1% BSA. Activation was initiated by adding TNP-BSA conjugate (30 µl, 2 µg/ml of TNP-BSA) as an activator. The plate was incubated at 37 °C for 30 min and then it was centrifuged for 5 min at 805 x g at 4 °C. 30 µl of each sample was mixed with 50 µl of 40 µM 4-methylumbelliferyl β-D-glucuronide and incubated for 60 min at 37 °C at the white plate. The reaction was stopped by adding 200 µl of ice-cold 0.2 M glycine buffer with pH 10.5 and fluorescence was measured with an Infinite 200M (TECAN) plate reader at 355 nm excitation and 460 nm emission wavelengths.

Cells which were used for determination of calcium response were sensitized as it was described for degranulation assay. Then the cells ($5x10^5$) were loaded with Fura-2-AM and probenecid to a final concentration 1 µM and 2.5 mM, respectively, and incubated for 20 min at 22 °C. After incubation, the cells were washed in BSS-BSA/probenecid and centrifuged at 805 x g for 5 min at 20 °C. After centrifugation they were suspended at concentration $5x10^5$/ml in BSS-BSA. Into white 96-well plate were inserted 100 µl aliquots. 100 µl of the activator (2 µg/ml of TNP-BSA) was added manually after 2 min of basal Ca^{2+} measurements. Changes in concentrations of intracellular Ca^{2+} were determined by spectrofluorometry using the Infinite 200M (TECAN) plate reader with excitation at 340 and 380 nm wavelengths and with a constant emission at 510 nm wavelength. Data are shown as a ratio $em510_{exc340}/em510_{exc380}$.

Reagents	Final con.	Volume/weight
HEPES	20 mM	2.38 g
NaCl	135 mM	3.94 g
KCl	5 mM	0.372 g
$CaCl_2.2H_2O$	1.8 mM	0.132 g
glucose	5.6 mM	0.5 g
dH_2O		Fill up to 0.5 L
Final volume		0,5 L

Table 8: BSS solution

Reagents	Con.	Volume/weight
BSA		10 mg
$MgCl_2$	1 M	10 µl
BSS		10 ml

Table 9: BSS-BSA solution

4.4 IMQ-induced dermatitis

For experiments were used 8-10-weeks-old female mice of WT, *Ormdl2* KO, *Ormdl3* KO and *Ormdl2&3* DKO genotype. The backs of mice were shaved with an electric shaver. Then, mice were treated with a daily dose of 62,5 mg IMQ-containing cream (Aldara; 5%) or common cream (Ambiderman) on the shaved back for up to 6 d. Mice were sacrificed on day 7 and the plasma and skin samples were collected.

4.5 Microscopy, histology and image analysis

All samples were examined in bright-field using a fluorescent microscope Leica DM6000 equipped with a color DFC490 camera.

Cytospin

Suspension of PDMCs (200 µl) was transferred on the microscope slide and centrifuged for 6 min at 40 x g. The slide was covered with 0.5% toluidine blue or Alcian blue/safranine (~1%) for 10 min after drying out the slide on air. After 10 min the slides were washed with distilled water three times, let dry on air, preserved with mounting medium (DPX Mountant for histology, Sigma), covered by cover slide and examined using X63/1.40 N.A. oil-immersion objective.

Histology

Samples from the skin of the murine back were used for histology. The samples were fixed 24h in 4% formaldehyde and then transferred to the 70% ethanol for minimum 24h. Next they were transferred to processor Leica ASP200S. After that, they were placed into a mold and coated with hot paraffin to form a blocks using Leica EG1150 H and let harden using Leica EG1150 C. Hard blocks of paraffin with the samples were placed into a microtome (Leica EM2255) and sliced into 5µm samples, which were placed into water bath (Leica HI1210) heated to 42 °C and let the paraffin stretched and smooth out. From the water bath, they were placed on the slide and let dry on Leica HI1220 heated to 42 °C. Dry slides were then deparaffinated and stained with Hematoxylin and eosin or Toluidine blue pH 2.3.

Deparaffinazitation: slides were washed three times per 8 min in Xylene, 5 min in 50/50 xylene/ethanol absolute, two times per 5 min in 100% ethanol, 3 min in 95% ethanol, 3 min in 70% ethanol and then washed in distilled water, then stained.

Staining for Hematoxylin and Eosin: slides were submerged into Hematoxylin for 3 min, washed in distilled water three times, submerged into Eosin for 3 min, then washed in distilled water three times, 20 s in 70% ethanol, 20 s in 90% ethanol, 1 min in 96% ethanol, and 3 min in xylene. Then let dry on air, fixed with mounting medium (DPX Mountant for histology), covered by cover slide, and examined using microscope Leica DM6000.

Staining for Toluidine blue: slides were submerged into 0.5% toluidine blue for 3 min, washed in distilled water three times, followed by ten dips in 95% ethanol, ten dips in 100% ethanol, and again ten dips in another 100% ethanol. Finally, the slides were submerged two times per 3 min in xylene. Then let dry on air, fixed with DPX Mountant for histology, covered by cover slide, and examined using microscope Leica DM6000.

Reagents	Volume/weight
Toluidine blue	1 g
70% ethanol	100 ml

Table 10: Toluidine blue stock solution

Reagents	Volume/weight
NaCl	0.5 g
dH2O	Fill up to 50 ml
Final volume	50 ml

Table 11: 1% NaCl ~2.3pH

Reagents	Volume
Toluidine blue stock solution	5 ml
1% NaCl, pH 2.3	45 ml
Final volume	50 ml

Table 12: 0.5% toluidine blue working solution

Reagents	Volume/weight
Alcian blue	900 mg
Safranine O	45 mg
Ferric ammonium sulphate	1.2 g
Acetate buffer	250 ml

Table 13: ~1% Alcian blue/safranin solution

4.6 List of chemicals and antigens

Reagent	Company	Identifier
4-methylumbelliferyl β-D-Glucuronide	Merck	89105
Alcian blue	SERVA	12020
Aldara™	Meda AB	
Ambiderman	E-laboratoř	
Ammonium persulfate	Merck	A3678-25G
B-mercaptoethanol	Merck	M3148
BSA	VWR	422361V
$CaCl_2.2H_2O$	Merck	223506
Couramic acid	Merck	C9008-5G
D-glucose	Merck	G8270
DPX Mountant for histology	Merck	06522
Dual color marker (10-250 kDa)	Bio-Rad	#1610374
Eosin	Merck	HT110216
Ethanol absolute	VWR	20821.296
Fetal bovine serum	Biosera	Cat# FB-1090/500
Formaldehyde	Merck	F-1268
Fura-2-AM	Merck	F0888
Glycine	Merck	G8898
Hematoxylin	Penta	39270-11000
HEPES	Merck	H-3784
Hydrogen peroxide	Fluka	95313
IL-3	Peprotech	#213-13
KCl	Merck	P9333
L-glutamine	Merck	G7513
Luminol	Merck	113072-5G
$MgCl_2$	Merck	M8266
MEM NEAA	Gibco	1114-035
NaCl	Merck	S3014
Paraffin wax	Bamed	B011008-03
PBS (8 g/l NaCl, 0.2 g/l KCl, 0.2 g/l KH_2PO_4, 1.15 g/l Na_2HPO_4) pH 7.4	IMG Core Facility – Media and Glass Washing	
Penicilin	Gibco	15140163
Polyacrylamide	Merck	92560-50G
Probenicid	Merck	P8761

RPMI	Merck	R8758
Safranin	Merck	1.15948
Sodium dodecyl sulfate	Merck	L3771
Skimmed milk	ELIGO Kolín	SV-SOM-ST
Sodium puryvate	Merck	P2256
Streptomycin	Merck	S6501
TNP-BSA conjugate	prepared in our laboratory	
Toluidine blue	Fluka	89640
Trizol® base	Merck	T1503
Tween	United States Biochemical	20605
TEMED	Merck	T9281
Xylen	Penta	28440-20010

Table 14: Table of chemicals and reagents

	Isotype	host	Company	Catalogue no
β-actin	IgG_1	Mouse	Santa Cruz Biotechnology	Sc-8432
HPRT	IgG_1	Mouse	Santa Cruz Biotechnology	sc-376938
IκB-α	Polyclonal serum	Rabbit	Santa Cruz Biotechnology	sc-371
p-IκB-α	IgG_1	Mouse	Cell Signaling	#9246
p-ERK	IgG	Rabbit	Santa Cruz Biotechnology	Tyr204; Sc-7976
SPTLC1	IgG_1	Mouse	Santa Cruz Biotechnology	sc-374143
SPTLC2	Polyclonal serum	Rabbit	Abcam. Antibodies	ab23696
pan-ORMDL	Polyclonal serum	Rabbit	Prepared in our laboratory, preparation described in Bugajev et al., 2016	
HRP- anti-rabbit	Polyclonal serum	Goat	Santa Cruz Biotechnology	sc-2005
HRP- anti-mouse	Polyclonal serum	Goat	Santa Cruz Biotechnology	sc-2004

Table 15: Table of used antigens

5 Results

5.1 To determine the role of ORMDL3 in peritoneal-derived mast cells (PDMCs) isolated from WT or *Ormdl3* KO mice.

Increased expression of ORMLD3 has been found in macrophages, eosinophils, T cells, lung epithelial cells and mast cells (Miller et al., 2012; Ha et al., 2013; Schmiedel et al., 2016, Bugajev 2016). The function of ORMDL3 in these cell types was described above in chapters 2.2.3.1 – 2.2.3.5. The combined data suggest that the changes in sphingolipid levels lead to the cell type specific responses. Therefore, it is important to study the role of ORMDL family in different tissues.

It was shown that ORMDL3 is a negative regulator of BMMCs signaling (Bugajev et al., 2016). In this study, BMMCs with ORMDL3 KD were used. To confirm the data and further extend them in *in vivo* studies, we prepared mice with *Ormdl3* KO using CRISPR/Cas9 technology. We isolated PDMCs from WT and *Ormdl3* KO mice, cultivated them and subsequently stained with Alcian blue/Safranin- and Toluidine blue to show that contains granules and are morphologically similar (Fig. 5).

To characterize the decrease in ORMDL family expression in PDMCs with *Ormdl3* KO, we prepared cell lysates from WT PDMCs and PDMCs with *Ormdl3* KO and assessed them by immunoblotting with the corresponding antibodies (Fig. 6a). Polyclonal serum used for ORMDL3 detection recognizes also other members of the ORMDL family therefore we observed only ~77% reduction in *Ormdl3* KO (Fig. 6b).

Degranulation is one of the most important effector function of mast cells (Galli et al., 2005). We examined the release of ß-glucuronidase, a marker of degranulation, into the supernatants of Ag-activated PDMCs isolated from WT or *Ormdl3* KO mice. We found that PDMCs with *Ormdl3* KO exhibited increased ß-glucuronidase release compared with WT PDMMCs (Fig. 7).

Next we measured calcium mobilization in PDMCs with *Ormdl3* KO. After the addition of activator, Ca^{2+} levels were measured for 6 min. As is shown in Fig. 8, Ca^{2+} response was enhanced in PDMCs with *Ormdl3* KO compared with WT PDMCs.

BMMCs with ORMDL3 KD exhibit increased phosphorylation of inhibitor of nuclear factor kappa B (IκB-α), accompanied by its degradation. This events initiates the NF-κB-dependent transcription of cytokines, chemokines, and COX2 (Bugajev et al., 2016). To determine the role of ORMDL3 in PDMCs IκB-α phosphorylation, we prepared cell lysates from non-activated and Ag-activated PDMCs isolated from WT and *Ormdl3* KO. We found that IκB-α was more phosphorylated in PDMCs with *Ormdl3* KO than in control cells. Moreover, the phosphorylation of extracellular signal-regulated protein kinase (ERK) was also increased in PDMCs isolated from *Ormdl3* KO mice compared with control PDMCs. Combined data suggest that ORMDL3 is a negative regulator of FcεRI-mediated signaling in PDMCs.

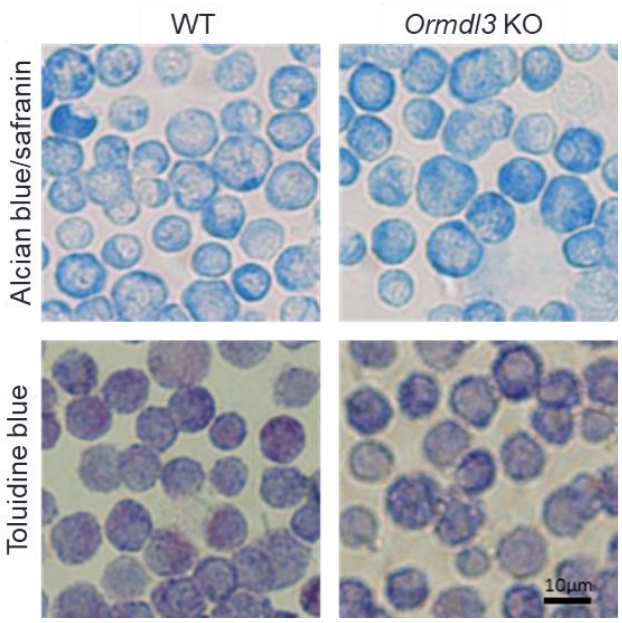

Fig. 5: Characterization of PDMCs derived from *Ormdl3* KO and WT mice

Alcian blue/Safranin and Toluidine blue staining of cytospin preparations of PDMCs WT and *Ormdl3* KO. Bar indicates 10 µm.

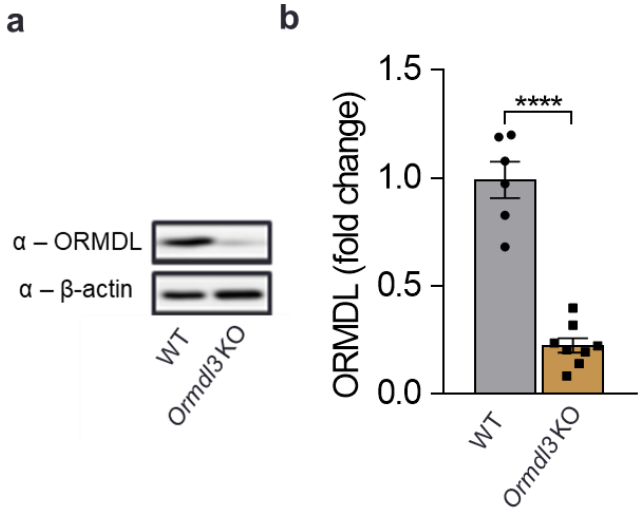

Fig. 6: Quantification of ORMDLs expression in WT and *Ormdl3* KO PDMCs.

a) Representative immunoblot of the lysates from PDMC isolated from WT and *Ormdl3* KO. **b)** Statistical analysis of ORMDL family expression normalized to expression in controls and β-actin load. WT ($n = 6$) and *Ormdl*3 KO ($n = 8$). Data shown as mean ± s.e.m., *n* shows number of independent experiments. Experiments were replicated at least three times. Data were compared with unpaired two sided Student's *t*-test, ****$P < 0.0001$.

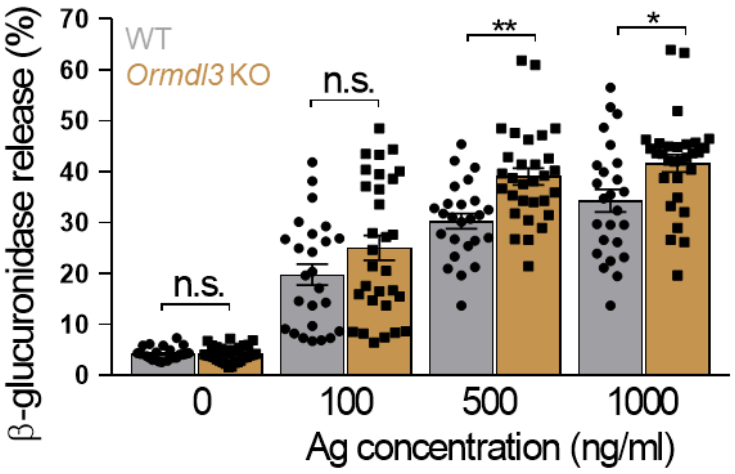

Fig. 7: Enhanced β-Glucuronidase release in PDMCs isolated from *Ormdl3* KO mice
Dose-dependent β-glucuronidase release into supernatants (30 min) of PDMCs WT (n = 25) and *Ormdl3* KO (n = 30) activated with various concentrations of Ag. Data shown as mean ± s.e.m., n shows number of independent experiments. Experiments replicated at least five times. Data were compared with unpaired two sided Student's t-test, **P < 0.01; *P < 0.05.

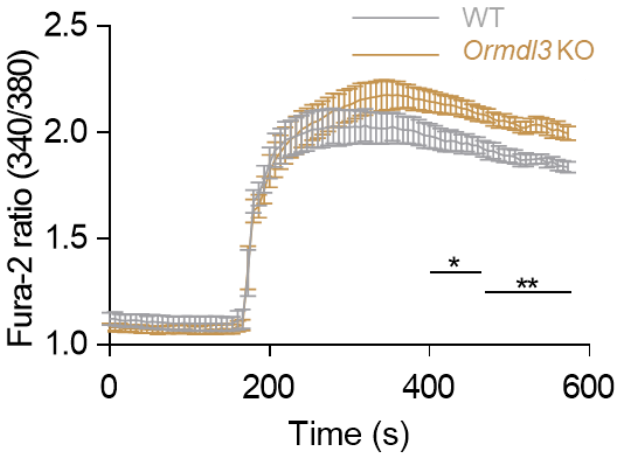

Fig. 8: Increased Ca^{2+} response in PDMCs isolated from *Ormdl3* KO
Calcium mobilization in PDMC WT (n = 7) and *Ormdl3* KO (n = 9) after activation with Ag (1µg/ml). Data shown as mean ± s.e.m., n shows number of independent experiments. Experiments replicated at least three times. Data were compared with unpaired two sided Student's t-test, **P < 0.01; *P < 0.05.

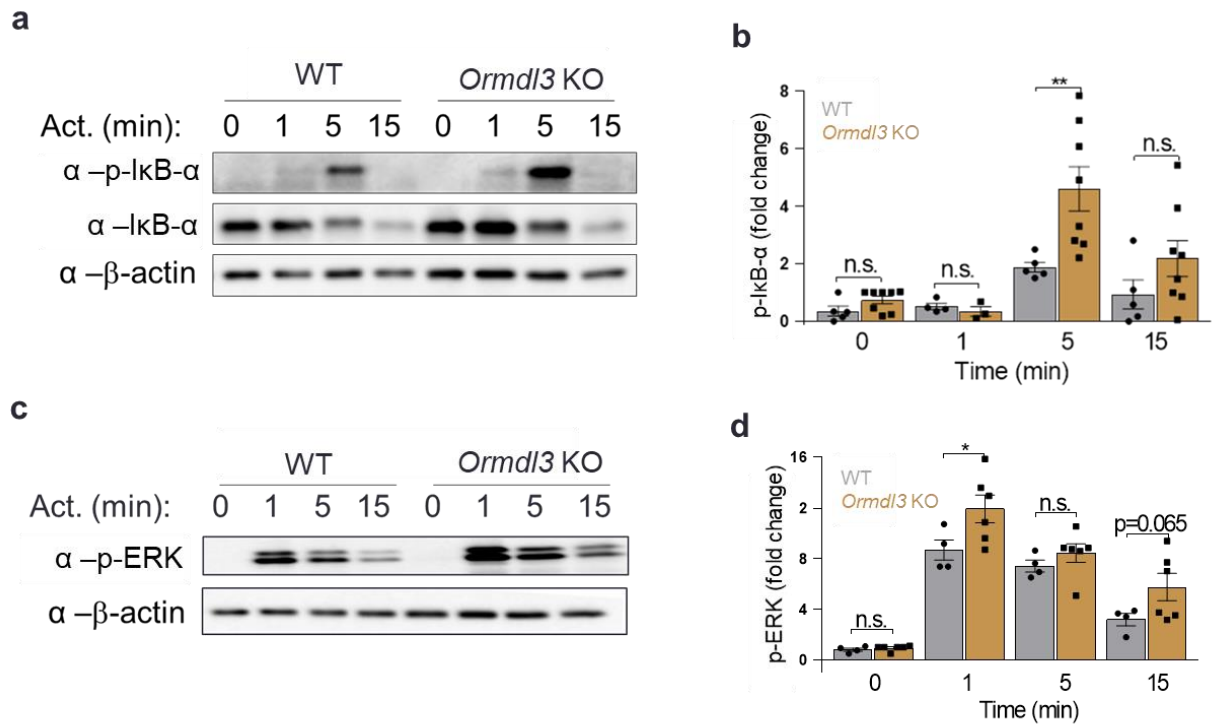

Fig. 9: Increased phosphorylation of IκB-α and ERK in PDMCs isolated from *Ormdl3* KO mice.

a) IκB-α phosphorylation (p-IκB-α) levels were determined by immunoblotting of whole-cell lysates from Ag-activated cells (TNP-BSA; 1 µg/ml) using the corresponding antibodies. **b)** Quantification and statistical evaluation of p-IκB-α normalized to non-activated PDMCs WT (n = 5) and *Ormdl3* KO (n = 8) and β-actin load. **c)** ERK phosphorylation (p-ERK) levels were determined by immunoblotting of whole-cell lysates from Ag-activated cells (TNP-BSA; 1 µg/ml) using the corresponding antibodies. **d)** Quantification and statistical evaluation of p-ERK normalized to non-activated PDMCs WT (n= 4) and *Ormdl3* KO (n= 6) and β-actin load. n shows number of independent experiments. Data shown as mean ± s.e.m. Data were compared by one-way ANOVA with Bonferoni post hoc test **P < 0.01; *P < 0.05.

5.2 Relationship between expression of ORMDL family and SPT complex

ORMDL proteins are regulators of SPT, first and rate limiting enzyme in *de novo* sphingolipid biosynthesis (Breslow et al., 2010; Wennekes et al., 2009; Wills-Karp, 2020). The decreased expression of SPT complex attenuates sphingolipid synthesis. On the other hand, lowered expression of ORMDLs increases sphingolipid levels. To test the hypothesis that the changes in expression of SPT complex and ORMDLs could be linked to maintain homeostasis of sphingolipids, we prepared SPTLC1 KD in BM-derived mast cell line (BMMCL) using lentiviral transduction. For analysis, polyclonal serum recognizing all members of ORMDL family and antibodies recognizing SPTLC1 and SPTLC2 were used. BMMCL with SPTLC1 KD exhibited reduced expression (~70%) of SPTLC1 compared with BMMCLs transduced with empty vector (control). Interestingly, decreased expression of SPTLC2 (~60%) and ORMDLs (~50%) were associated with SPTLC1 KD (Fig. 10a-d). These data suggested that the expression of SPTLC2 and ORMDLs depends on SPTLC1 levels.

To study the role of decreased ORMDL levels on SPTLC1 and SPTLC2 expression, we used BMMCs isolated from WT, *Ormdl2* KO, *Ormdl3* KO, and *Ormdl2&3* DKO mice. Cell lysates of these BMMCs were prepared and analyzed using immunoblotting. The expression of ORMDL family proteins is decreased down to ~20% in *Ormdl2&3* DKO mice and ~40% in *Ormdl3* KO mice (Fig. 11a, b). The expressions of SPTLC1 and SPTLC2 are independent of missing ORMDL2 and/or ORMDL3.

These data showed that silencing of SPTLC1 decreases also the expression of SPTLC2 and ORMDLs. However, the absence of ORMDL2 and/or ORMDL3 does not have an impact on the expression of SPTLC1 and SPTLC2.

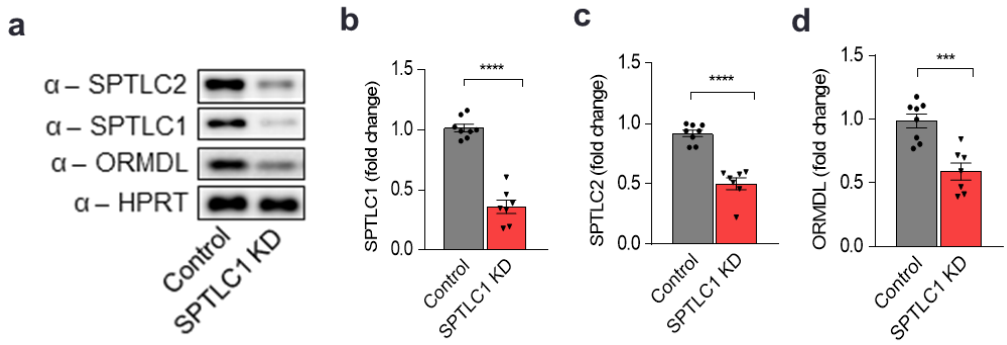

Fig. 10: Analysis of BMMC with SPTLC1 KD.

a) Representative immunoblot of the lysates from BMMCL transduced with empty vector (Control) or SPTLC1 shRNA (SPTLC1 KD) were assessed by immunoblotting. **b-d)** Quantification of data as in Fig. 10a, normalized to expression in controls and HPRT load. Controls (n = 9), SPTLC1 KD (n = 7). Data shown as mean ± s.e.m., n shows number of independent experiments. Data were compared with unpaired two sided Student's t-test, ***P < 0.001; ****P < 0.0001.

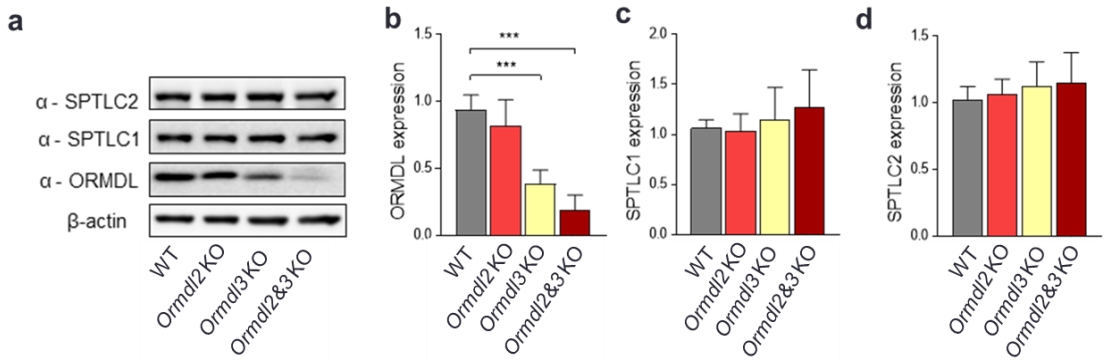

Fig. 11: Characterization of the ORMDL family member's expression in BMMCs isolated from *Ormdl2* KO, *Ormdl3* KO and *Ormdl2&3* DKO.

a) Representative immunoblot of the lysates from BMMCs isolated from WT or *Ormdl2* KO, *Ormdl3* KO, and *Ormdl2&3* DKO mice was developed with pan-ORMDL-specific antibody and the antibodies recognizing long chain subunits of the serine palmytoil transferase (SPT) complex. **(b-d)** Statistical analysis of the data presented in Fig. 11a, normalized to expression of β-actin and control (WT) cells; PDMCs with WT (n = 6), *Ormdl2* KO (n = 6), *Ormdl3* KO (n = 6), and *Ormdl2&3* DKO (n = 6). Data shown as mean ± s.e.m., n shows number of independent experiments. Data were compared by one-way ANOVA with Bonferoni post hoc test ***P < 0.001

5.3 The role of ORMDL family in IMQ-induced dermatitis

Changes in the production of various ceramides have been associated with the differentiation of keratinocytes, and thereby the development of a normal skin barrier, with secondary implications on the pathogenesis of psoriasis and atopic dermatitis (Fishelevich et al., 2004; Lew et al., 2006; Ishikawa et al., 2010). Compared with healthy controls, sera of patients with psoriasis exhibit increased levels of S1P and decreased levels of ceramide (Myśliwiec et al., 2017). In concordance, pharmacological inhibition of S1P production in mice ameliorates IMQ-induced dermatitis (Shin et al., 2019). These data suggest that the regulation of sphingolipid synthesis is important in psoriasis and IMQ-induced dermatitis. Therefore, we tested the hypothesis that ORMDLs are involved in IMQ-induced dermatitis.

To this aim we established IMQ-induced dermatitis as a model of psoriasis-like dermatitis in mice. We used WT, *Ormdl2* KO, *Ormdl3* KO, and *Ormdl2&3* DKO. These mice were treated with IMQ or common moisturizing cream (controls) for 6 days. Mice were sacrificed on day 7 and photographed for visual comparison (Fig. 12). The body weight of these mice was on day 7 comparable among all groups (Fig. 13a). However, the spleen weights increased in all IMQ-treated mice compared with control groups (Fig. 13b). When we normalized the spleen weight to the terminal body weight of corresponding mice, we obtained similar results (Fig 13c).

Next, histological samples were analyzed. Hematoxylin-eosin staining was used to visualize swelling of the skin (Fig. 14a). Thickness of the epidermis and/or dermis was determined using the LAS AF Lite software (Fig. 14b, c). These data suggest that *Ormdl2&3* DKO mice exhibit decreased swelling compared with WT mice. Thus, ORMDLs may have a role in the reduction of swelling in IMQ-induced dermatitis. We also stained the histological samples with toluidine blue, which is used for the identification of mast cells (Fig 15a, b).

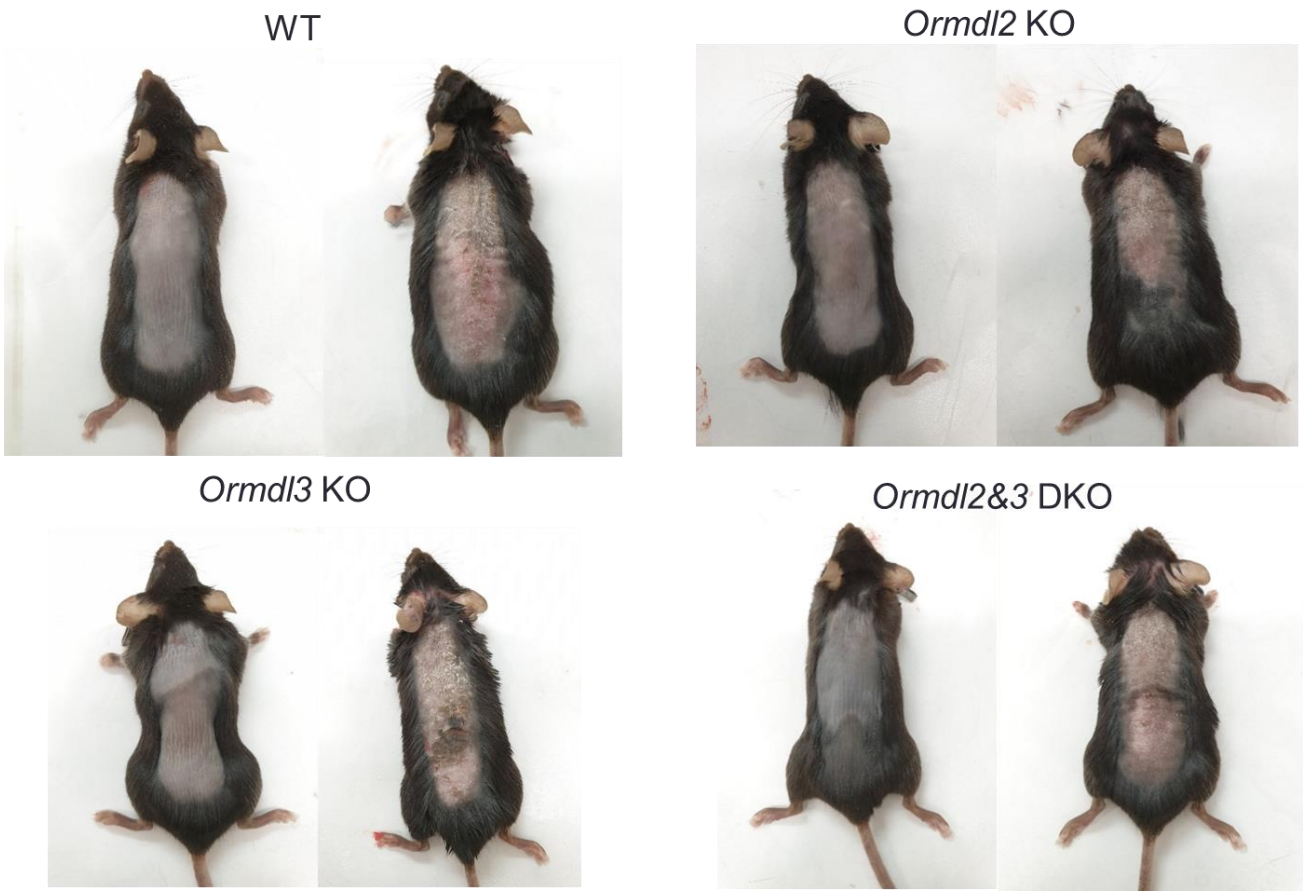

Fig. 12: IMQ-induced dermatitis in WT, *Ormdl2* KO, *Ormdl3* KO and *Ormdl2&3* DKO mice.

Mice were treated with IMQ or common moisturizing cream (controls) for 6 days. Mice were sacrificed on day 7 and photographed for visual comparison. In each group (WT, *Ormdl2* KO, *Ormdl3* KO, and *Ormdl2&3* DKO) are on the left mice treated with common cream (controls) and on the right IMQ-treated mice.

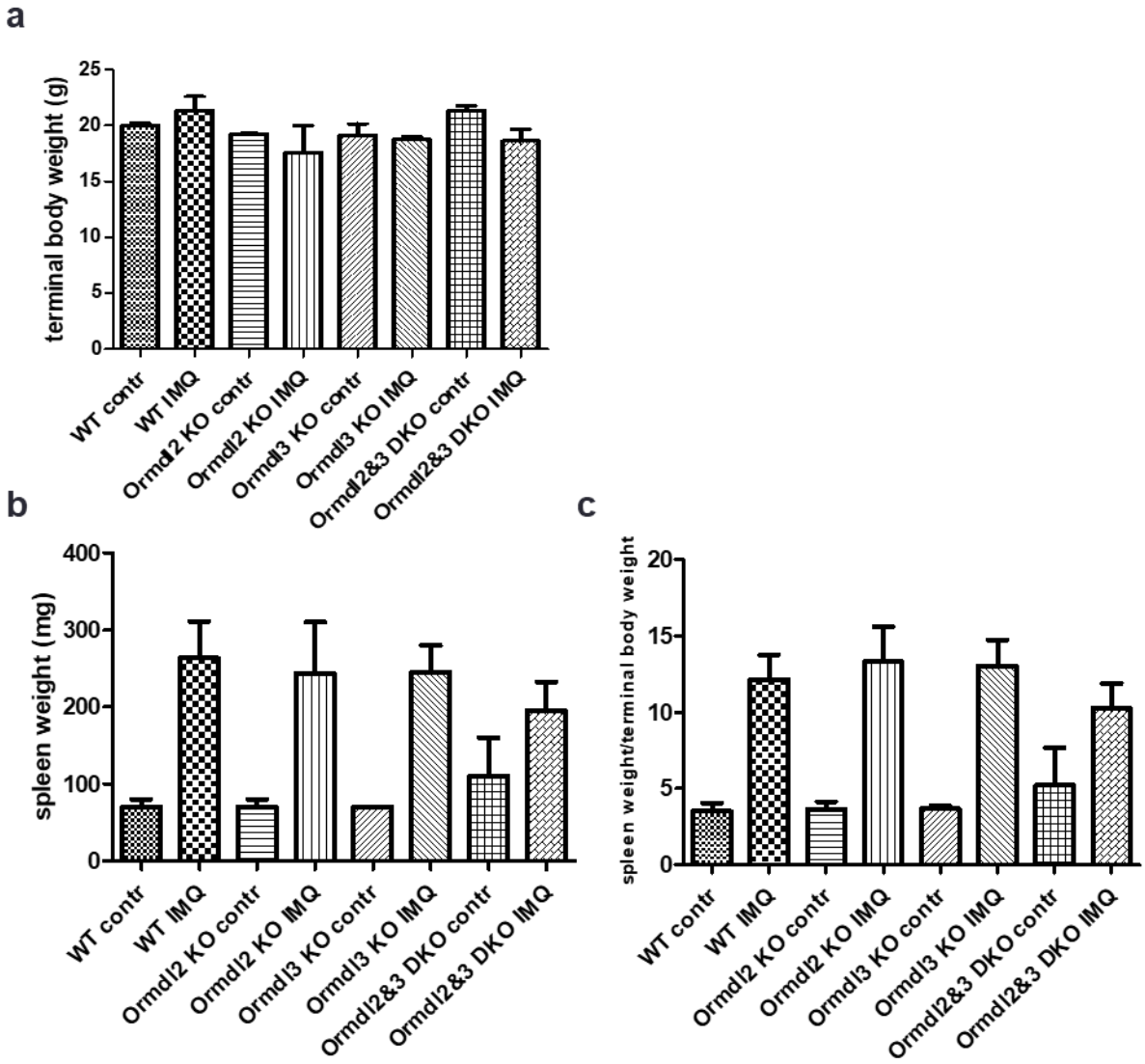

Fig. 13: Terminal body and spleen weight in WT, *Ormdl2* KO, *Ormdl3* KO, and *Ormdl2&3* DKO mice treated with common cream (control) or IMQ cream

a) Mice weight on day 7 (the last day of experiment). **b)** Spleens were collected and weight. **c)** The ratio of spleen weight to terminal body weight. WT contr. (*n*=2), WT IMQ (*n*=3), *Ormdl2* KO contr. (*n* = 2), *Ormdl2* KO IMQ (*n*= 3), *Ormdl3* KO contr. (*n*=2), *Ormdl3* KO IMQ (*n*=2), *Ormdl2&3* DKO contr. (*n*=2) and *Ormdl2&3* DKO IMQ (*n*=4). Data shown as mean ± s.e.m., *n* shows number of number of biological replicates.

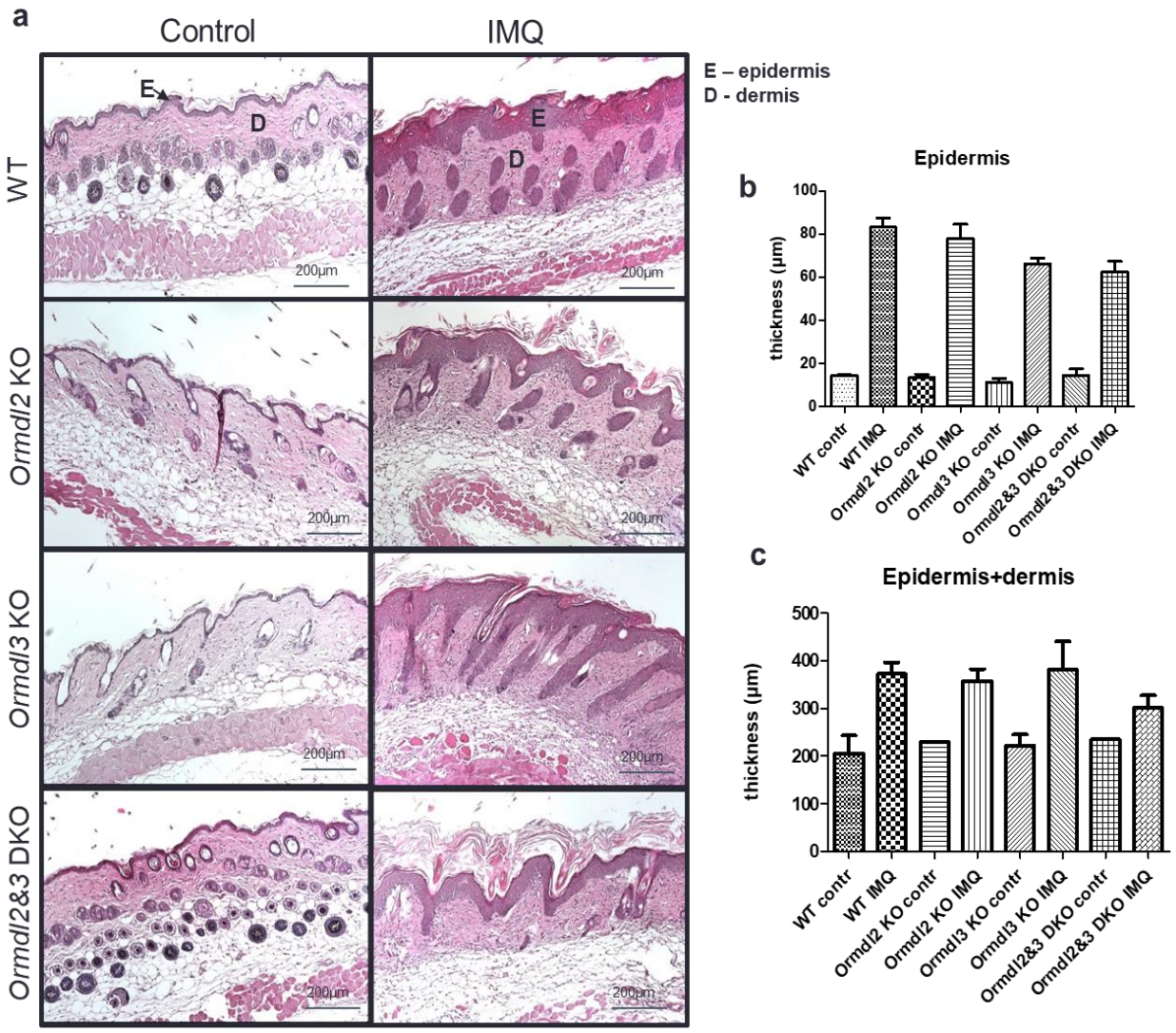

Fig. 14: IMQ-dependent thickening of epidermis and/or dermis in WT, *Ormdl2* KO, *Ormdl3* KO and *Ormdl2&3* DKO mice. a) Hematoxylin and eosin staining of the skin. Skin tissue was collected from murine back on day 7. **b)** Analysis of the data presented in a. Bar indicates 200 µm. WT contr. (*n*=2), WT IMQ (*n*=3), *Ormdl2* KO contr. (*n*= 2), *Ormdl2* KO IMQ (*n*= 3), *Ormdl3* KO contr. (*n*=2), *Ormdl3* KO IMQ (*n*=2), *Ormdl2&3* DKO contr. (*n*=2) and *Ormdl2&3* DKO IMQ (*n*=4). Data shown as mean ± s.e.m., *n* shows number of biological replicates.

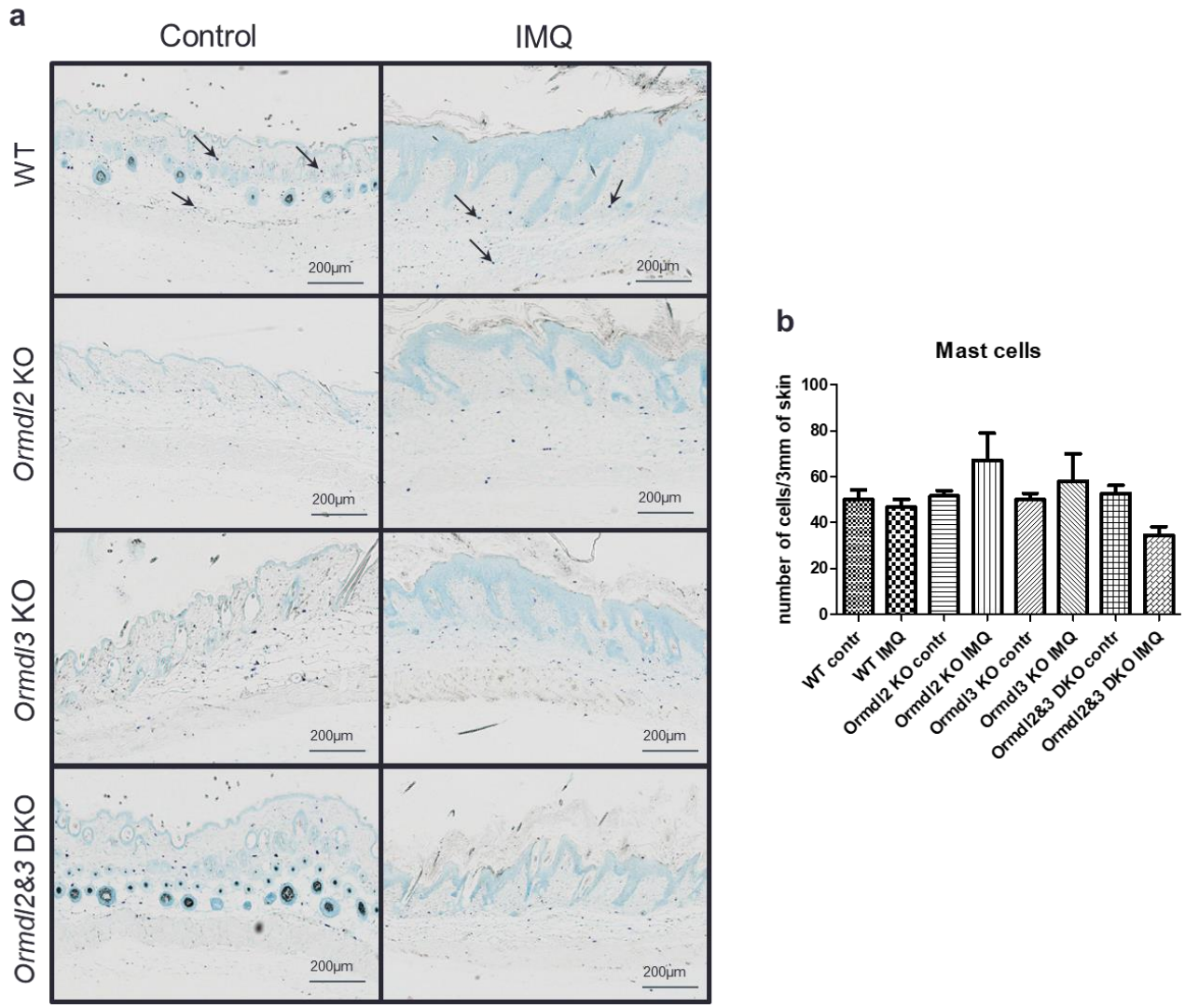

Fig. 15: Mast cell counts in the skin of mice treated with common cream (control) and mice treated with IMQ

a) Toluidine blue staining of the skin. Tissue was collected from murine back on day 7. **b)** Analysis of the data presented in a, number of mast cells per 3mm^2 of the skin. Bar indicates 200 µm. The arrowheads point to the mast cells. Mast cells were counted using LAS AF Lite software. WT contr. (*n*=2), WT IMQ (*n*=3), *Ormdl2* KO contr. (*n*= 2), *Ormdl2* KO IMQ (*n*= 3), *Ormdl3* KO contr. (*n*=2), *Ormdl3* KO IMQ (*n*=2), *Ormdl2&3* DKO contr. (*n*=2) and *Ormdl2&3* DKO IMQ (*n*=4). Data shown as mean ± s.e.m., *n* shows number of biological replicates.

6 Discussion

SNPs in the chromosome 17q12-q21 region were associated with risk of asthma and other inflammatory diseases such as primary biliary cirrhosisn Crohn's disease, rheumatoid arthritis and type 1 diabetes. In the same chromosome is localized *ORMDL3*. ORMDL3 is a highly conserved transmembrane protein and a negative regulator of *de novo* sphingolipid synthesis (Moffatt et al., 2007; Verlaan et al., 2009; Breslow et al., 2010; Kurreeman et al., 2012). *De novo* sphingolipid synthesis is mediated by SPT, which is a complex of SPTLC1 and STLC2 or SPTLC3 subunits (Mandon et al., 1991; Hanada, 2003; Breslow et al., 2010; Siow et al., 2015; Harrison et al., 2018). The changes in sphingolipid synthesis are crucial in cellular events such as apoptosis, proliferation and differentiation (Hannun and Luberto, 2000). Literature data suggest, that the changes in sphingolipid levels exhibit the cell type specific responses (Miller et al., 2012; Ha et al., 2013; Schmiedel et al., 2016, Bugajev 2016). It is, therefore, important to study the sphingolipid biosynthesis pathway in different cell types.

The aims of this thesis were to determine the roles of ORMDL3 in FcεRI-induced signaling, analyze the relationship between expression of ORMDL family and SPT complex and study the role of ORMDL family in IMQ-induced dermatitis.

In the first part, we showed that PDMCs isolated from WT and *Ormdl3* KO mice exhibited comparable morphological properties of mast cells. Western blot analysis comparing PDMC lysates from WT and *Ormdl3* KO mice showed that ORMDL3 is abundantly expressed in ORMDL family. The expression of the other two ORMDLs in lysates from PDMCs with *Ormdl3* KO was ~20%. Moreover, the expression of *Ormdl1* and *Ormdl2* transcripts in PDMCs with *Ormdl3* KO was comparable with WT PDMCs (Bugajev et al. manuscript in preparation).

Previous study showed that Ag-activated BMMCs with reduced or enhanced ORMDL3 expression did not exhibit changes in calcium response or degranulation when compared with control cells (Bugajev et al., 2016). However, experiments performed using PDMCs isolated from *Ormdl3* KO mice showed an increase in Ag-induced degranulation and calcium response compared with WT PDMCs. Previously, it was shown that Ag-activated BMMCs with ORMDL3 KD exhibit the increased phosphorylation of IκB-α but not ERK. Therefore

we used PDMCs with O*rmdl3* KO to study Ag-induced phosphorylation of IκB-α and ERK. We found that after Ag activation, PDMCs isolated from *Ormdl3* KO mice exhibited increased phosphorylation of IκB-α and ERK compared with PDMCs from WT mice. Phosphorylation of IκB-α in ORMDL3-deficient PDMCs resulted in increased production of TNF-α (not shown; Bugajev et al. manuscript in preparation). These data suggest that ORMDL3-dependent changes in degranulation, calcium mobilization and ERK phosphorylation are strictly associated with the ORMDL3 levels and that the remaining expression of ORMDL3 in ORMDL3 KD limits them.

As was previously mentioned, ORMDL proteins regulate the SPT activity (Breslow et al., 2010; Davis et al., 2019b). Recently, it was shown that ORMDLs exhibit redundant function (Clarke et al., 2019). Zhakupova et al., (2016) showed that ORMDL3 overexpression did not have a role in production of sphingolipids. However, Oyeniran et al., (2015) showed that the role of ORMDL3 in sphingolipid synthesis could dependent on the concentration of vectors coding ORMDL3. Moreover, the silencing of all three members of ORMDL family in Hela or HEK293 caused the increased production of sphingolipids (Breslaw et al., 2010; Siow and Wattenberg, 2012; Zhakupova et al, 2016). These data suggest that the sphingolipid synthesis in different tissues depends on the ratio of ORMDL family members.

To test the hypothesis that the changes in the expression of SPT complex and ORMDLs could be linked together to maintain sphingolipid homeostasis, we prepared SPTLC1 KD in BMMCL. The levels of ORMDLs, SPTLC1, and SPTLC2 in SPTLC1 KD were determined. We found that the levels of ORMDLs (~50%), SPTLC1 (~30%) and SPTLC2 (~60%) were decreased in SPTLC1 KD BMMCL compared with control cells. However, in BMMCs isolated from *Ormdl2* KO, *Ormdl3* KO and *Ormdl2&3* DKO mice the expression of SPTLC1 and SPTLC2 was comparable with their expression in WT BMMCs. In BMMCs, the remaining expression of ORMDL family proteins was significantly altered only in BMMCs with *Ormdl3* KO (~40%) and *Ormdl2&3* DKO (~80%). Differences in the levels of the remaining members of the ORMDL family in *Ormdl3* KO BMMCs (Fig. 6) and PDMCs (Fig 11a, b) could be explained by distinct expression ratios of the ORMDL family members in these mast cell types. The decreased levels of SPTLC2 and ORMDLs in BMMCL with SPTLC1 KD suggest the there is a regulatory mechanism to maintain the ratio of SPT-ORMDLs levels. These results correspond with the increased expression of ORMDLs in cells overexpressing the SPT complex (Gupta et al., 2015).

The changes in sphingolipid synthesis are associated with diseases, such as dermatitis. Recently, it was shown that the decreased levels of S1P production in mice ameliorates IMQ-induced dermatitis accompanied by reduced psoriasis-like skin symptoms (Shin et al., 2019). Ag-activated mast cells also generate and release S1P. S1P regulates mast cell signaling (Olivera et al., 2010). Recently, IMQ-induced dermatitis was connected to mast cell-dependent pseudo-allergic reaction. It was shown that MRGPRB2 receptor on mast cells is important for IMQ-induced dermatitis development (Hao et al., 2020; McNeil et al., 2015).

These data suggest that the ORMDL family-dependent regulation of sphingolipid synthesis could be important in IMQ-induced dermatitis. Therefore we tested the hypothesis that ORMDLs are involved in IMQ-induced dermatitis. For this experiment we used WT, *Ormdl2* KO*, Ormdl3* KO, *Ormdl2&3* DKO mice. In summary, we successfully established the model of IMQ-induced dermatitis in our lab (Fig. 13, Fig. 14). It should be noted that we performed a pilot experiment, therefore we don´t have enough data to statistically analyze them. However, the preliminary data suggest that ORMDLs may play a role in the pathogenesis of IMQ-induced dermatitis.

7 Conclusions

Aim 1: To determinate the role of ORMDL3 in peritoneal-derived mast cells (PDMCs) isolated from WT or *Ormdl3* KO mice.

a. The PDMCs isolated from *Ormdl3* KO and WT mice exhibited properties of mast cells.

b. PDMCs with depleted ORMDL3 exhibited residual expression (~20%) of other members of ORMDL family.

c. β-glucuronidase release was enhanced in PDMCs isolated from *Ormdl3* KO mice compared with WT mice.

d. Calcium response was enhanced in PDMCs isolated from *Ormdl3* KO mice compared with WT mice.

e. PDMCs isolated from *Ormdl3* KO mice exhibited increased phosphorylation of IκB-α and ERK.

Aim 2: To analyze the relationship between expression of ORMDL family and SPT complex.

a. Silencing of SPTLC1 decreased the expression of SPTLC2 and ORMDLs in BMMCL.
b. The absence of ORMDL2 and/or ORMDL3 did not have an impact on the expression of SPTLC1 and SPTLC2 in BMMCs.

Aim 3: To study the role of ORMDL family in the IMQ-induced dermatitis.

Preliminary data suggested that ORMDLs may play a role in the pathogenesis of IMQ-induced dermatitis.

8 References

Arinobu, Y., Iwasaki, H., Gurish, M. F., Mizuno, S., Shigematsu, H., Ozawa, H., Tenen, D. G., Austen, K. F., & Akashi, K. (2005). Developmental checkpoints of the basophil/mast cell lineages in adult murine hematopoiesis. *Proceedings of the National Academy of Sciences of the United States of America,* 102(50), 18105–18110.

Bischoff S. C. (2007). Role of mast cells in allergic and non-allergic immune responses: comparison of human and murine data. *Nature reviews. Immunology*, *7*(2), 93–104.

Breslow D. K., Collins S. R., Bodenmiller B., Aebersold R., Simons K., Shevchenko A., Ejsing C. S., and Weissman J. S. (2010) Orm family proteins mediate sphingolipid homeostasis. *Nature* 463, 1048–1053.

Bugajev, V., Halova, I., Draberova, L., Bambouskova, M., Potuckova, L., Draberova, H., Paulenda, T., Junyent S., & Petr Draber (2016) Negative regulatory roles of ORMDL3 in the FcεRI-triggered expression of proinflammatory mediators and chemotactic response in murine mast cells. *Cellular and Molecular Life Sciences*. 73, 1265–1285

Clarke, B. A., Majumder, S., Zhu, H., Lee, Y. T., Kono, M., Li, C., Khanna, C., Blain, H., Schwartz, R., Huso, V. L., Byrnes, C., Tuymetova, G., Dunn, T. M., Allende, M. L., & Proia, R. L. (2019). The *Ormdl* genes regulate the sphingolipid synthesis pathway to ensure proper myelination and neurologic function in mice. *eLife*, *8*, e51067.

da Silva, E. Z., Jamur, M. C., & Oliver, C. (2014). Mast cell function: a new vision of an old cell. *The journal of histochemistry and cytochemistry: official journal of the Histochemistry Society*, *62*(10), 698–738.

Das, S., Miller, M., & Broide, D. H. (2017). Chromosome 17q21 genes ORMDL3 and GSDMB in asthma and immune diseases. *Advances in immunology*, *135*, 1–52.

Davis, D. L., Gable, K., Suemitsu, J., Dunn, T. M., & Wattenberg, B. W. (2019b) The ORMDL/Orm-serine palmitoyltransferase (SPT) complex is directly regulated by ceramide: Reconstitution of SPT regulation in isolated membranes. *The Journal of biological chemistry*, *294*(13), 5146–5156.

Davis, D., Suemitsu, J., & Wattenberg, B. (2019a) Transmembrane topology of mammalian ORMDL proteins in the endoplasmic reticulum as revealed by the substituted cysteine accessibility method (SCAM™). *Biochimica et biophysica acta. Proteins and proteomics*, *1867*(4), 382–395.

Debeuf, N., Zhakupova, A., Steiner, R., Van Gassen, S., Deswarte, K., Fayazpour, F., Van Moorleghem, J., Vergote, K., Pavie, B., Lemeire, K., Hammad, H., Hornemann, T., Janssens, S., & Lambrecht, B. N. (2019). The ORMDL3 asthma susceptibility gene regulates systemic ceramide levels without altering key asthma features in mice. *The Journal of allergy and clinical immunology*, *144*(6), 1648–1659.e9.

Dileepan, M., Ha, S. G., Rastle-Simpson, S., Ge, X. N., Greenberg, Y. G., Wijesinghe, D. S., Contaifer, D., Jr, Rao, S. P., & Sriramarao, P. (2020). Pulmonary delivery of ORMDL3 short hairpin RNA - a potential tool to regulate allergen-induced airway inflammation. *Experimental lung research*, *46*(7), 243–257.

Fishelevich, R., Malanina, A., Luzina, I., Atamas, S., Smyth, M. J., Porcelli, S. A., & Gaspari, A. A. (2006). Ceramide-dependent regulation of human epidermal keratinocyte CD1d expression during terminal differentiation. *Journal of immunology* (Baltimore, Md.: 1950), 176(4), 2590–2599.

Futerman, A.H., Hannun, Y.A. (2004) The complex life of simple sphingolipids, *EMBO* Rep.5 777–782.

Galli SJ, Tsai M, Piliponsky AM (2008) The development of allergic inflammation. *Nature* 454:445–454.

Galli, S. J., Nakae, S., & Tsai, M. (2005). Mast cells in the development of adaptive immune responses. *Nature immunology*, *6*(2), 135–142.

Gilfillan, A. M., & Tkaczyk, C. (2006). Integrated signalling pathways for mast-cell activation. *Nature reviews. Immunology*, *6*(3), 218–230.

Gilfillan, A. M., Peavy, R. D., & Metcalfe, D. D. (2009). Amplification mechanisms for the enhancement of antigen-mediated mast cell activation. *Immunologic research*, *43*(1-3), 15–24.

Gupta, S. D., Gable, K., Alexaki, A., Chandris, P., Proia, R. L., Dunn, T. M., & Harmon, J. M. (2015). Expression of the ORMDLS, modulators of serine palmitoyltransferase, is regulated by sphingolipids in mammalian cells. The Journal of biological chemistry, 290(1), 90–98.

Ha, S. G., Ge, X. N., Bahaie, N. S., Kang, B. N., Rao, A., Rao, S. P., & Sriramarao, P. (2013). ORMDL3 promotes eosinophil trafficking and activation via regulation of integrins and CD48. *Nature communications*, 4, 2479.

Hamid, Q., & Tulic, M. (2009). Immunobiology of asthma. *Annual review of physiology*, *71*, 489–507.

Han G, Gupta SD, Gable K, Niranjanakumari S, Moitra P, Eichler F, Brown RH, Jr., Harmon JM, and Dunn TM. (2009) 'Identification of small subunits of mammalian serine palmitoyltransferase that confer distinct acyl-CoA substrate specificities', *Proceedings of the National Academy of Sciences of the United States of America,* 106: 8186–91.

Hanada K. (2003) Serine palmitoyltransferase, a key enzyme of sphingolipid metabolism. *Biochimica et biophysica acta*, 1632(1-3), 16–30.

Hannun, Y. A., & Obeid, L. M. (2008). Principles of bioactive lipid signalling: lessons from sphingolipids. *Nature reviews. Molecular cell biology*, *9*(2), 139–150.

Hannun, Y.A., Luberto, C. (2000) Ceramide in the eukaryotic stress response, *Trends in Cell Biology.,* 10 pp. 73-80.

Hao, Y., Peng, B., Che, D., Zheng, Y., Kong, S., Liu, R., Shi, J., Han, H., Wang, J., Cao, J., Zhang, Y., Gao, J., He, L., & Geng, S. (2020). Imiquimod-related dermatitis is mainly mediated by mast cell degranulation via Mas-related G-protein coupled receptor B2. *International immunopharmacology*, *81*, 106258.

Harrison, P. J., Dunn, T. M., & Campopiano, D. J. (2018). Sphingolipid biosynthesis in man and microbes. *Natural product reports*, 35(9), 921–954.

Hjelmqvist, L., Tuson, M., Marfany, G., Herrero, E., Balcells, S., & Gonzàlez-Duarte, R. (2002) ORMDL proteins are a conserved new family of endoplasmic reticulum membrane proteins. *Genome biology*, 3(6), RESEARCH0027.

Ishikawa, J., Narita, H., Kondo, N., Hotta, M., Takagi, Y., Masukawa, Y., Kitahara, T., Takema, Y., Koyano, S., Yamazaki, S., & Hatamochi, A. (2010). Changes in the ceramide profile of atopic dermatitis patients. *The Journal of investigative dermatology*, 130(10), 2511–2514.

Jolly, P. S., Bektas, M., Olivera, A., Gonzalez-Espinosa, C., Proia, R. L., Rivera, J., Milstien, S., & Spiegel, S. (2004). Transactivation of sphingosine-1-phosphate receptors by FcepsilonRI triggering is required for normal mast cell degranulation and chemotaxis. *The Journal of experimental medicine*, *199*(7), 959–970.

Kiefer, K., Carreras-Sureda, A., García-López, R., Rubio-Moscardó, F., Casas, J., Fabriàs, G., & Vicente, R. (2015). Coordinated regulation of the orosomucoid-like gene family expression controls *de novo* ceramide synthesis in mammalian cells. *The Journal of biological chemistry*, *290*(5), 2822–2830.

Kiefer, K., Casas, J., García-López, R., & Vicente, R. (2019). Ceramide imbalance and impaired TLR4-mediated autophagy in BMDM of an ORMDL3-overexpressing mouse model. *International journal of molecular sciences*, *20*(6), 1391.

Kinet J. P. (1999). The high-affinity IgE receptor (Fc epsilon RI): from physiology to pathology. *Annual review of immunology*, *17*, 931–972.

Kovářová, M., Tolar, P., Arudchandran, R., Dráberová, L., Rivera, J., & Dráber, P. (2001). Structure-function analysis of Lyn kinase association with lipid rafts and initiation of early signaling events after Fcepsilon receptor I aggregation. *Molecular and cellular biology*, *21*(24), 8318–8328.

Kunder, C. A., St John, A. L., Li, G., Leong, K. W., Berwin, B., Staats, H. F., & Abraham, S. N. (2009). Mast cell-derived particles deliver peripheral signals to remote lymph nodes. *The Journal of experimental medicine*, *206*(11), 2455–2467.

Kurreeman FA, Stahl EA, Okada Y, Liao K, Diogo D, Raychaudhuri S, Freudenberg J, Kochi Y, Patsopoulos NA, Gupta N; CLEAR investigators, Sandor C, Bang SY, Lee HS, Padyukov L, Suzuki A, Siminovitch K, Worthington J, Gregersen PK, Hughes LB, Reynolds RJ, Bridges SL Jr, Bae SC, Yamamoto K, Plenge RM. (2012) Use of a multiethnic approach to identify rheumatoid- arthritis-susceptibility loci, 1p36 and 17q12. *The American Journal of Human Genetics.* 90:524–532.

Lew, B. L., Cho, Y., Kim, J., Sim, W. Y., & Kim, N. I. (2006). Ceramides and cell signaling molecules in psoriatic epidermis: reduced levels of ceramides, PKC-alpha, and JNK. *Journal of Korean medical science,* 21(1), 95–99.

Lim, D. H., Cho, J. Y., Miller, M., McElwain, K., McElwain, S., & Broide, D. H. (2006). Reduced peribronchial fibrosis in allergen-challenged MMP-9-deficient mice. *American journal of physiology. Lung cellular and molecular physiology*, *291*(2), L265–L271.

Löser, S., Gregory, L. G., Zhang, Y., Schaefer, K., Walker, S. A., Buckley, J., Denney, L., Dean, C. H., Cookson, W., Moffatt, M. F., & Lloyd, C. M. (2017). Pulmonary ORMDL3 is critical for induction of Alternaria-induced allergic airways disease. *The Journal of allergy and clinical immunology*, *139*(5), 1496–1507.e3.

Lowther, J., Naismith, J. H., Dunn, T. M., & Campopiano, D. J. (2012). Structural, mechanistic and regulatory studies of serine palmitoyltransferase. *Biochemical Society transactions*, *40*(3), 547–554.

Mandon E. C., van Echten G., Birk R., Schmidt R. R., and Sandhoff K. (1991) Sphingolipid biosynthesis in cultured neurons: down-regulation of serine palmitoyltransferase by sphingoid bases. *European Journal of Biochemistry.* 198, 667–674.

Marshall J. S. (2004). Mast-cell responses to pathogens. *Nature reviews. Immunology*, *4*(10), 787–799.

McNeil, B. D., Pundir, P., Meeker, S., Han, L., Undem, B. J., Kulka, M., & Dong, X. (2015). Identification of a mast-cell-specific receptor crucial for pseudo-allergic drug reactions. *Nature*, *519*(7542), 237–241.

Miller, M., Rosenthal, P., Beppu, A., Mueller, J. L., Hoffman, H. M., Tam, A. B., Doherty, T. A., McGeough, M. D., Pena, C. A., Suzukawa, M., Niwa, M., & Broide, D. H. (2014) ORMDL3 transgenic mice have increased airway remodeling and airway responsiveness characteristic of asthma. *Journal of immunology (Baltimore, Md.: 1950)*, *192*(8), 3475–3487.

Miller, M., Tam, A. B., Cho, J. Y., Doherty, T. A., Pham, A., Khorram, N., Rosenthal, P., Mueller, J. L., Hoffman, H. M., Suzukawa, M., Niwa, M., & Broide, D. H. (2012). ORMDL3 is an inducible lung epithelial gene regulating metalloproteases, chemokines, OAS, and ATF6. *Proceedings of the National Academy of Sciences of the United States of America,* 109(41), 16648–16653.

Miller, M., Tam, A. B., Mueller, J. L., Rosenthal, P., Beppu, A., Gordillo, R., McGeough, M. D., Vuong, C., Doherty, T. A., Hoffman, H. M., Niwa, M., & Broide, D. H. (2017). Cutting Edge: Targeting Epithelial ORMDL3 Increases, Rather than Reduces, Airway Responsiveness and Is Associated with Increased Sphingosine-1-Phosphate. *Journal of immunology (Baltimore, Md.: 1950)*, *198*(8), 3017–3022.

Moffatt MF, Kabesch M, Liang L, Dixon AL, Strachan D, Heath S, Depner M, von Berg A, Bufe A, Rietschel E, Heinzmann A, Simma B, Frischer T, Willis-Owen SA, Wong KC, Illig T, Vogelberg C, Weiland SK, von Mutius E, Abecasis GR, Farrall M, Gut IG, Lathrop GM, and Cookson WO. (2007) 'Genetic variants regulating ORMDL3 expression contribute to the risk of childhood asthma', *Nature*, 448: 470–73.

Myśliwiec, H., Baran, A., Harasim-Symbor, E., Choromańska, B., Myśliwiec, P., Milewska, A. J., Chabowski, A., & Flisiak, I. (2017). Increase in circulating sphingosine-1-phosphate and decrease in ceramide levels in psoriatic patients. *Archives of dermatological research*, *309*(2), 79–86.

Naus, S., Blanchet, M. R., Gossens, K., Zaph, C., Bartsch, J. W., McNagny, K. M., & Ziltener, H. J. (2010). The metalloprotease-disintegrin ADAM8 is essential for the development of experimental asthma. *American journal of respiratory and critical care medicine*, *181*(12), 1318–1328.

Ohno, I., Ohtani, H., Nitta, Y., Suzuki, J., Hoshi, H., Honma, M., Isoyama, S., Tanno, Y., Tamura, G., Yamauchi, K., Nagura, H., & Shirato, K. (1997). Eosinophils as a source of matrix metalloproteinase-9 in asthmatic airway inflammation. *American journal of respiratory cell and molecular biology*, *16*(3), 212–219.

Olivera A. (2008). Unraveling the complexities of sphingosine-1-phosphate function: the mast cell model. *Prostaglandins & other lipid mediators*, *86*(1-4), 1–11.

Olivera, A., Eisner, C., Kitamura, Y., Dillahunt, S., Allende, L., Tuymetova, G., Watford, W., Meylan, F., Diesner, S. C., Li, L., Schnermann, J., Proia, R. L., & Rivera, J. (2010). Sphingosine kinase 1 and sphingosine-1-phosphate receptor 2 are vital to recovery from anaphylactic shock in mice. *The Journal of clinical investigation*, *120*(5), 1429–1440.

Ono, J. G., Kim, B. I., Zhao, Y., Christos, P. J., Tesfaigzi, Y., Worgall, T. S., & Worgall, S. (2020). Decreased sphingolipid synthesis in children with 17q21 asthma-risk genotypes. *The Journal of clinical investigation*, *130*(2), 921–926.

Oyeniran, C., Sturgill, J. L., Hait, N. C., Huang, W. C., Avni, D., Maceyka, M., Newton, J., Allegood, J. C., Montpetit, A., Conrad, D. H., Milstien, S., & Spiegel, S. (2015). Aberrant ORM (yeast)-like protein isoform 3 (ORMDL3) expression dysregulates ceramide homeostasis in cells and ceramide exacerbates allergic asthma in mice. *The Journal of allergy and clinical immunology*, *136*(4), 1035–46.e6.

Paulissen, G., Rocks, N., Guéders, M. M., Bedoret, D., Crahay, C., Quesada-Calvo, F., Hacha, J., Bekaert, S., Desmet, C., Foidart, J. M., Bureau, F., Noel, A., & Cataldo, D. D. (2011). ADAM-8, a metalloproteinase, drives acute allergen-induced airway inflammation. *European journal of immunology*, *41*(2), 380–391.

Perry D. K. (2000). The role of *de novo* ceramide synthesis in chemotherapy-induced apoptosis. *Annals of the New York Academy of Sciences*, *905*, 91–96.

Possa, S. S., Leick, E. A., Prado, C. M., Martins, M. A., & Tibério, I. F. (2013). Eosinophilic inflammation in allergic asthma. *Frontiers in pharmacology*, 4, 46.

Rudolph, A. K., Burrows, P. D., & Wabl, M. R. (1981). Thirteen hybridomas secreting hapten-specific immunoglobulin E from mice with Iga or Igb heavy chain haplotype. *European journal of immunology*, *11*(6), 527–529.

Schmiedel, B. J., Seumois, G., Samaniego-Castruita, D., Cayford, J., Schulten, V., Chavez, L., Ay, F., Sette, A., Peters, B., & Vijayanand, P. *(2016). 17q21 asthma-risk variants switch CTCF binding and regulate IL-2 production by T cells. Nature communications, 7, 13426.*

Seals, D. F., & Courtneidge, S. A. (2003). The ADAMs family of metalloproteases: multidomain proteins with multiple functions. *Genes & development*, *17*(1), 7–30.

Shin, S. H., Cho, K. A., Hahn, S., Lee, Y., Kim, Y. H., Woo, S. Y., Ryu, K. H., Park, W. J., & Park, J. W. (2019). Inhibiting Sphingosine Kinase 2 Derived-sphingosine-1-phosphate Ameliorates Psoriasis-like Skin Disease via Blocking Th17 Differentiation of Naïve CD4 T Lymphocytes in Mice. *Acta dermato-venereologica*, *99*(6), 594–601.

Siow D. L., and Wattenberg B. W. (2012) Mammalian ORMDL proteins mediate the feedback response in ceramide biosynthesis. *J. Biol. Chem*. 287, 40198–40204

Siow, D., Sunkara, M., Dunn, T. M., Morris, A. J., & Wattenberg, B. (2015). ORMDL/serine palmitoyltransferase stoichiometry determines effects of ORMDL3 expression on sphingolipid biosynthesis. *Journal of lipid research*, *56*(4), 898–908.

Stone, K. D., Prussin, C., & Metcalfe, D. D. (2010). IgE, mast cells, basophils, and eosinophils. *The Journal of allergy and clinical immunology*, *125*(2 Suppl 2), S73–S80.

Tkaczyk, C., Horejsi, V., Iwaki, S., Draber, P., Samelson, L. E., Satterthwaite, A. B., Nahm, D. H., Metcalfe, D. D., & Gilfillan, A. M. (2004). NTAL phosphorylation is a pivotal link between the signaling cascades leading to human mast cell degranulation following Kit activation and Fc epsilon RI aggregation. *Blood*, 104(1), 207–214.

Tkaczyk, C., Jensen, B. M., Iwaki, S., & Gilfillan, A. M. (2006). Adaptive and innate immune reactions regulating mast cell activation: from receptor-mediated signaling to responses. *Immunology and allergy clinics of North America*, *26*(3), 427–450.

Tsai, M., Takeishi, T., Thompson, H., Langley, K. E., Zsebo, K. M., Metcalfe, D. D., Geissler, E. N., & Galli, S. J. (1991). Induction of mast cell proliferation, maturation, and heparin synthesis by the rat c-kit ligand, stem cell factor. *Proceedings of the National Academy of Sciences of the United States of America,* 88(14), 6382–6386.

Verlaan DJ, Berlivet S, Hunninghake GM, Madore AM, Larivière M, Moussette S, Grundberg E, Kwan T, Ouimet M, Ge B, Hoberman R, Swiatek M, Dias J, Lam KC, Koka V, Harmsen E, Soto-Quiros M, Avila L, Celedón JC, Weiss ST, Dewar K, Sinnett D, Laprise C, Raby BA, Pastinen T, Naumova AK. (2009) Allele-specific chromatin remodeling in the ZPBP2/GSDMB/ORMDL3 locus associated with the risk of asthma and autoimmune disease. *The American Journal of Human Genetics* 85:377–393.

Wennekes, T., van den Berg, R. J., Boot, R. G., van der Marel, G. A., Overkleeft, H. S., & Aerts, J. M. (2009). Glycosphingolipids--nature, function, and pharmacological modulation. *Angewandte Chemie (International ed. in English)*, *48*(47), 8848–8869.

Wills-Karp M. (2020). At last - linking ORMDL3 polymorphisms, decreased sphingolipid synthesis, and asthma susceptibility. *The Journal of clinical investigation*, 130(2), 604–607.

Zhakupova, A., Debeuf, N., Krols, M., Toussaint, W., Vanhoutte, L., Alecu, I., Kutalik, Z., Vollenweider, P., Ernst, D., von Eckardstein, A., Lambrecht, B. N., Janssens, S., & Hornemann, T. (2016). ORMDL3 expression levels have no influence on the activity of serine palmitoyltransferase. *FASEB journal: official publication of the Federation of American Societies for Experimental Biology*, *30*(12), 4289–4300.